# Forward-central two-particle correlations in p–Pb collisions at √sNN = 5.02 TeV

(ALICE Collaboration) Adam, J.; ...; Antičić, Tome; ...; Erhardt, Filip; ...; Gotovac, Sven; ...; Mudnić, Eugen; ...; ...

Source / Izvornik: Physics Letters B, 2016, 753, 126 - 139

Journal article, Published version
Rad u časopisu, Objavljena verzija rada (izdavačev PDF)

https://doi.org/10.1016/j.physletb.2015.12.010

Physics Letters B 753 (2016) 126–139

Contents lists available at ScienceDirect

Physics Letters B

www.elsevier.com/locate/physletb

# Forward-central two-particle correlations in p–Pb collisions at $\sqrt{s_{NN}} = 5.02$ TeV

ALICE Collaboration *

ARTICLE INFO

*Article history:*
Received 15 July 2015
Received in revised form 30 November 2015
Accepted 4 December 2015
Available online 8 December 2015
Editor: L. Rolandi

ABSTRACT

Two-particle angular correlations between trigger particles in the forward pseudorapidity range ($2.5 < |\eta| < 4.0$) and associated particles in the central range ($|\eta| < 1.0$) are measured with the ALICE detector in p–Pb collisions at a nucleon–nucleon centre-of-mass energy of 5.02 TeV. The trigger particles are reconstructed using the muon spectrometer, and the associated particles by the central barrel tracking detectors. In high-multiplicity events, the double-ridge structure, previously discovered in two-particle angular correlations at midrapidity, is found to persist to the pseudorapidity ranges studied in this Letter. The second-order Fourier coefficients for muons in high-multiplicity events are extracted after jet-like correlations from low-multiplicity events have been subtracted. The coefficients are found to have a similar transverse momentum ($p_T$) dependence in p-going (p–Pb) and Pb-going (Pb–p) configurations, with the Pb-going coefficients larger by about $16 \pm 6\%$, rather independent of $p_T$ within the uncertainties of the measurement. The data are compared with calculations using the AMPT model, which predicts a different $p_T$ and $\eta$ dependence than observed in the data. The results are sensitive to the parent particle $v_2$ and composition of reconstructed muon tracks, where the contribution from heavy flavour decays is expected to dominate at $p_T > 2$ GeV/$c$.



## 1. Introduction

Measurements of correlations in $\Delta\varphi$ and $\Delta\eta$, where $\Delta\varphi$ and $\Delta\eta$ are the differences in azimuthal angle ($\varphi$) and pseudorapidity ($\eta$) between two particles, respectively, provide insight on the underlying mechanism of particle production in collisions of hadrons and nuclei at high energy.

For such measurements in proton–proton (pp) collisions, jet production leads to a characteristic peak-like structure on the "near side" (at $\Delta\varphi \approx 0$, $\Delta\eta \approx 0$) and an elongated structure in $\Delta\eta$ on the "away side" (at $\Delta\varphi \approx \pi$) [1]. In nucleus–nucleus (A–A) collisions, ridge-like structures extending over a long range along the $\Delta\eta$ axis emerge on the near and away sides, in addition to the jet-related correlations [2–14]. The Fourier decomposition of the correlation in $\Delta\varphi$ at large $\Delta\eta$ is dominated by the second- and third-order harmonic coefficients $v_2$ and $v_3$, but significant harmonics have been measured up to $v_6$ [6,7,9–16]. In A–A collisions, the $v_n$ coefficients are interpreted as the collective response of the created matter to the collision geometry and fluctuations in the initial state [17,18], and are used to extract its transport properties in hydrodynamic models [19–21].

Long-range ridge structures on the near side ($\Delta\varphi \approx 0$) were also observed in high-multiplicity pp collisions at a centre-of-mass energy $\sqrt{s} = 7$ TeV [22] and in proton–lead (p–Pb) collisions at a nucleon–nucleon centre-of-mass energy $\sqrt{s_{NN}} = 5.02$ TeV [23]. Shortly after, measurements in which the contributions from jet fragmentation were suppressed by subtracting the correlations extracted from low-multiplicity events revealed the presence of essentially the same long-range structures on the away side as on the near side in high-multiplicity events [24,25]. Evidence of long-range double-ridge structures in high-multiplicity deuteron–gold (d–Au) collisions at $\sqrt{s_{NN}} = 0.2$ TeV was also reported [26]. By now, the existence of long-range correlations in p–Pb collisions is firmly established by measurements [27–31] involving four, six or more particle correlations, with the lower-order correlations removed [32], demonstrating that the long-range ridges originate from genuine multi-particle correlations. Intriguingly, the transverse momentum dependence of the extracted $v_n$ [27,28,30], and the particle-mass dependence of $v_n$ [33–35] are found to be qualitatively similar to those measured in A–A collisions.

The similarity of the ridges in the pp, p–Pb, d–Au and A–A systems suggests the possibility of a common hydrodynamical origin [36–43]. However, whether hydrodynamical models can indeed be reliably applied to such small systems is under intense debate [44]. Other proposed mechanisms involve initial-state effects, such as gluon saturation and extended color connections forming

* E-mail address: alice-publications@cern.ch.

http://dx.doi.org/10.1016/j.physletb.2015.12.010

along the longitudinal direction [45–49] or final-state parton–parton induced interactions [50–54].

Further insight into the production mechanism of these long-range correlation structures may be gained by studying their $\eta$-dependence. A preliminary result [55] indicates a mild $\eta$ dependence, but the measurement is limited to $|\eta| < 2$. A similar magnitude of the two-particle correlation amplitudes in the Au-going and d-going directions at $2.8 < |\eta| < 3.8$ has also been reported in d–Au collisions at $\sqrt{s_{\rm NN}} = 0.2$ TeV [56]. Calculations for $v_2$ at large $\eta$ ($2.5 < |\eta| < 4$) in p–Pb collisions at $\sqrt{s_{\rm NN}} = 5.02$ TeV from a $3 + 1$ dimensional, viscous hydrodynamical model and a multi-phase transport model (AMPT) predict a stronger $\eta$ dependence, with about 50% and 30% larger $v_2$ values on the lead nucleus side for the hydrodynamical and AMPT model, respectively [57].

In this Letter, we report a measurement of angular correlations between trigger particles in the pseudorapidity range $2.5 < |\eta| < 4.0$ and associated particles in the central range $|\eta| < 1.0$ in p–Pb collisions at $\sqrt{s_{\rm NN}} = 5.02$ TeV at the Large Hadron Collider (LHC). The trigger particles are inclusive muons, reconstructed using the ALICE muon spectrometer, and the associated particles are charged particles, reconstructed by the ALICE central barrel tracking detectors. As in previous measurements [24,33], the double ridge is extracted by subtracting the correlations obtained in low-multiplicity events from those in high-multiplicity events. Results for the second order Fourier coefficient for muons, $v_2^{\mu}\{\rm 2PC, sub\}$, and the ratio of $v_2^{\mu}\{\rm 2PC, sub\}$ coefficients[1] in the Pb-going (Pb–p) and p-going (p–Pb) directions are reported for high-multiplicity events, and compared to model predictions. The remainder of the Letter is structured as follows: We describe the experimental setup in Sec. 2, the event and track selection in Sec. 3, the analysis method in Sec. 4 and the evaluation of the systematic uncertainties in Sec. 5. Finally, in Sec. 6 we report the results, and compare them with model predictions. In Sec. 7 we conclude with a summary.

## 2. Experimental setup

In 2013, the LHC provided collisions between protons with a beam energy of 4 TeV and lead ions with a beam energy of 1.58 TeV per nucleon, resulting in a centre-of-mass energy of $\sqrt{s_{\rm NN}} = 5.02$ TeV. The beams were set up in two configurations: a period with the proton momentum in the direction of negative $\eta$ in the ALICE coordinate system, denoted as p–Pb, followed by a period with reversed beams, denoted as Pb–p. Due to the asymmetric beam energies, the nucleon–nucleon centre-of-mass reference system moves with a rapidity of 0.465 in the direction of the proton beam with respect to the ALICE laboratory system. Pseudorapidity, denoted by $\eta$, is given in the laboratory frame throughout this Letter.

Details on ALICE and its subdetectors can be found in Refs. [58, 59]. In the following, we give a brief summary of the components needed for the measurement reported in the Letter.

Trigger tracks used in this analysis are detected in the muon spectrometer with an acceptance of $-4.0 < \eta < -2.5$. The muon spectrometer consists of a thick absorber of about ten interaction lengths ($\lambda_{\rm I}$), which filters muons in front of five tracking stations made of two planes of Cathode Pad Chambers each. The third station is placed inside a dipole magnet with a 3 Tm integrated field. The tracking apparatus is completed by a trigger system made of four layers of Resistive Plate Chambers placed behind a second absorber of 7.2 $\lambda_{\rm I}$ thickness. This setup ensures that most of the hadrons in the acceptance are stopped in one of the absorber layers, providing a muon purity above 99% for the tracks used in this analysis. In p–Pb collisions, the trigger particle travels in the same direction as the p beam (p-going case), while in Pb–p collisions in the same direction as the Pb nucleus (Pb-going case).

Associated particles in $|\eta| < 1.0$ are reconstructed using the combined information from the Inner Tracking System (ITS) and the Time Projection Chamber (TPC), which are located inside the ALICE solenoid with a field of 0.5 T. The ITS consists of six layers of silicon detectors: two layers of Silicon Pixel Detector (SPD), surrounded by two layers of Silicon Drift Detector (SDD) and two layers of Silicon Strip Detector (SSD). SPD tracklets, short track segments reconstructed in the two SPD layers alone, are also used as associated particles.

The V0 detector, consisting of two arrays with 32 scintillator tiles arranged in four rings each, is used to generate the minimum-bias trigger and offline for multiplicity selection [60]. The detector covers the full azimuth within $2.8 < \eta < 5.1$ (V0-A) and $-3.7 < \eta < -1.7$ (V0-C). The timing information of the V0 is also used for offline rejection of interactions of the beam with residual gas. In addition, two neutron Zero Degree Calorimeters (ZDCs) located at $+112.5$ m (ZNA) and $-112.5$ m (ZNC) from the interaction point are used in the offline event selection and as an alternative approach to define event-multiplicity classes.

## 3. Event and track selection

The online event selection used in this analysis is based on a combination of minimum-bias (MB) and muon trigger inputs. The MB selection uses the coincidence between hits in the V0-A and V0-C detectors and covers 99.2% of the non-single-diffractive cross section as described in [61]. Only approximately 5% of the MB events contain one or more tracks reconstructed in the muon spectrometer. In order to increase the number of recorded events, the presence of at least one muon above a $p_{\rm T}$ threshold was required in addition to the MB trigger condition. Two different thresholds were used: a low-$p_{\rm T}$ threshold corresponding to about 0.5 GeV/$c$ ($\mu$-low-$p_{\rm T}$) and a higher $p_{\rm T}$ threshold corresponding to about 4.2 GeV/$c$ ($\mu$-high-$p_{\rm T}$). These thresholds are not sharp and the reported values correspond to a 50% trigger probability for a muon candidate. The integrated luminosity collected with $\mu$-high-$p_{\rm T}$ triggers is 5.0 nb$^{-1}$ in the p–Pb and 5.8 nb$^{-1}$ in the Pb–p periods. The $\mu$-low-$p_{\rm T}$ trigger class was downscaled by a factor 10–35 depending on the data taking conditions, resulting in an integrated luminosity of 0.28 nb$^{-1}$ in the p–Pb and 0.26 nb$^{-1}$ in the Pb–p periods.

The TPC and SDD detectors have longer deadtime compared to the muon spectrometer, the SPD and the V0. Therefore, they were read out only in a fraction of $\mu$-low-$p_{\rm T}$ events (about 25% in p–Pb and below 10% in Pb–p collisions). Both muon-track and muon-tracklet correlation results were measured in the p–Pb configuration. For Pb–p collisions, only muon-tracklet correlations could be studied due to the significantly lower number of triggers with the TPC in the readout.

The primary-vertex position is determined using reconstructed clusters in the SPD detector as described in Ref. [59]. Only events with a reconstructed vertex coordinate along the beam direction ($z_{\rm vtx}$) within 7 cm from the nominal interaction point are selected. The probability of multiple interactions in the same bunch crossing (pileup) was dependent on the beam conditions and always below 3%. Pileup events are removed by rejecting triggers with more than one reconstructed vertex.

All events were characterized by their event activity, and sorted into event classes. As in previous studies [24,33], the event characterization was based on the signal in the V0 detectors. However,

[1] Here, and in the following, "2PC" stands for "two-particle correlation" and "sub" for "subtraction", and indicates the analysis technique with which the coefficients are measured.

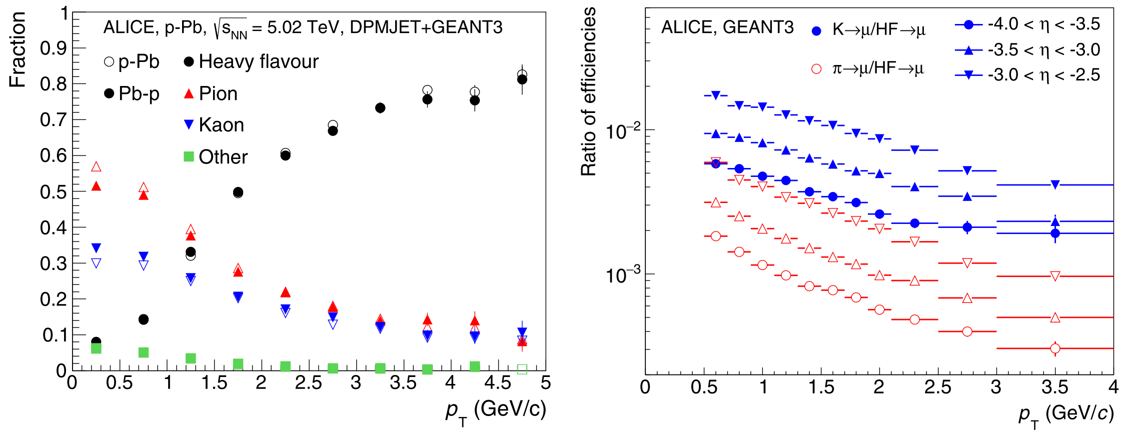


**Fig. 1.** Parent particle composition of reconstructed muon tracks (left panel) and reconstruction efficiency for muons from pion and kaon decays relative to that for heavy flavor (HF) decay muons (right panel) from a detector simulation of the ALICE muon spectrometer.

**Table 1**
V0S multiplicity classes as fractions of the analyzed event sample and the corresponding $\langle dN_{ch}/d\eta\rangle|_{|\eta|<0.5}$. The $\langle dN_{ch}/d\eta\rangle$ values are not corrected for trigger and vertex-reconstruction inefficiencies, which are about 4% for non-single-diffractive events [61], mainly affecting the 80–100% lowest mulitiplicity events [62]. Only systematic uncertainties are listed, since the statistical uncertainties are negligible.

| Event class | $\langle dN_{ch}/d\eta\rangle|_{|\eta|<0.5}$ $p_T >$ 0 GeV/$c$ |
|---|---|
| 0–20% | $35.8 \pm 0.8$ |
| 20–40% | $23.2 \pm 0.5$ |
| 40–60% | $15.8 \pm 0.4$ |
| 60–100% | $6.8 \pm 0.2$ |

unlike before, both beam orientations were investigated in this Letter. Therefore, the signals from only two out the four rings of V0-A and V0-C detectors were combined to guarantee a more symmetric acceptance. On the V0-A side, the two outermost rings with an acceptance of $2.8 < \eta < 3.9$, while on the V0-C side the two innermost rings with an acceptance of $-3.7 < \eta < -2.7$ were used. This combination is called V0S in the following. The definition of the event classes as fractions of the analyzed event sample and their corresponding average number of particles at midrapidity ($\langle dN_{ch}/d\eta\rangle|_{|\eta|<0.5}$), measured using tracklets as explained below, is given in Table 1.

Muon tracks are reconstructed in the geometrical acceptance of the muon spectrometer ($-4 < \eta < -2.5$). The tracks are required to exit the front absorber at a radial distance from the beam axis, $R_{abs}$, in the range $17.6 < R_{abs} < 89.5$ cm in order to avoid regions with large material density. The muon identification is performed by matching the tracks reconstructed in the tracking chambers with the corresponding track segments in the trigger chambers. Beam-gas tracks, which do not point to the interaction vertex, are removed by a selection on the product of the total momentum of a given track and its distance to the interaction vertex in the transverse plane. In the analysis, muons in the transverse momentum range $0.5 < p_T < 4$ GeV/$c$ were considered.

Reconstructed muons mainly originate from weak decays of $\pi$, K[2] and mesons from heavy flavor (HF) decays. Because of the different $p_T$ distribution of the various sources and the absorber in front of the spectrometer, which suppresses by design weak decays from light hadrons, the parent particle composition for the reconstructed muon tracks changes as a function of $p_T$. The composition shown as a function of the reconstructed $p_T$ in the left panel of Fig. 1 was evaluated using full detector simulations based on the DPMJET Monte Carlo (MC) event generator [63]. The detector response was simulated using GEANT3 for particle transport [64]. The composition of parent particles in the simulation differs by less than 10% for the two beam configurations. The reconstructed muons are dominated by light-hadron decays below 1.5 GeV/$c$, and by heavy flavor decays above 2 GeV/$c$. No significant multiplicity dependence was found. Similar conclusions are obtained using simulations with the AMPT generator [65].

Without strong model assumptions, one cannot deduce the composition of parent particles from the measured muon distribution, and correct the data for muon decay and absorber effects. For comparison of the $v_2$ data with calculations, however, only relative contributions of the parent species matter. In order to ease future model calculations, the reconstruction efficiencies for muons from pion and kaon decays relative to those for muons from heavy flavor decays are provided in the right panel of Fig. 1 as a function of the generated decay muon $p_T$ in different pseudorapidity intervals. Contributions from muon decays of other particles are significantly smaller than those for pions and can be ignored. The systematic uncertainty on the relative efficiencies was estimated to be less than 5%.

Tracks reconstructed in the ITS and the TPC are selected in the fiducial region $|\eta| < 1$ and $0.5 < p_T < 4$ GeV/$c$. The track selection used in this Letter is the same as in Ref. [24].

Tracklet candidates are formed using information on the position of the primary vertex and the two hits on the SPD layers [66], located at a distance of 3.9 and 7.6 cm from the detector centre. The differences of the azimuthal ($\Delta\varphi_h$, bending plane) and polar ($\Delta\theta_h$, non-bending direction) angles of the hits with respect to the primary vertex are used to select particles, typically with $p_T > 50$ MeV/$c$. Particles below 50 MeV/$c$ are mostly absorbed by material. Compared to previous analyses [61,66] a tighter cut in $\Delta\varphi_h$ is applied ($\Delta\varphi_h < 5$ mrad) to select particles with larger $p_T$ and to minimize contributions of fake and secondary tracks to below 2.5%. The corresponding mean $p_T$ of selected particles, estimated from the DPMJET MC, is about 0.75 GeV/$c$.

## 4. Analysis

The associated yield of tracks or tracklets per trigger particle in the muon spectrometer is measured as a function of the difference

[2] Here, and in the following, pions and kaons refer to the sum of both charge states. Neutral particles are also considered in the case of kaons.

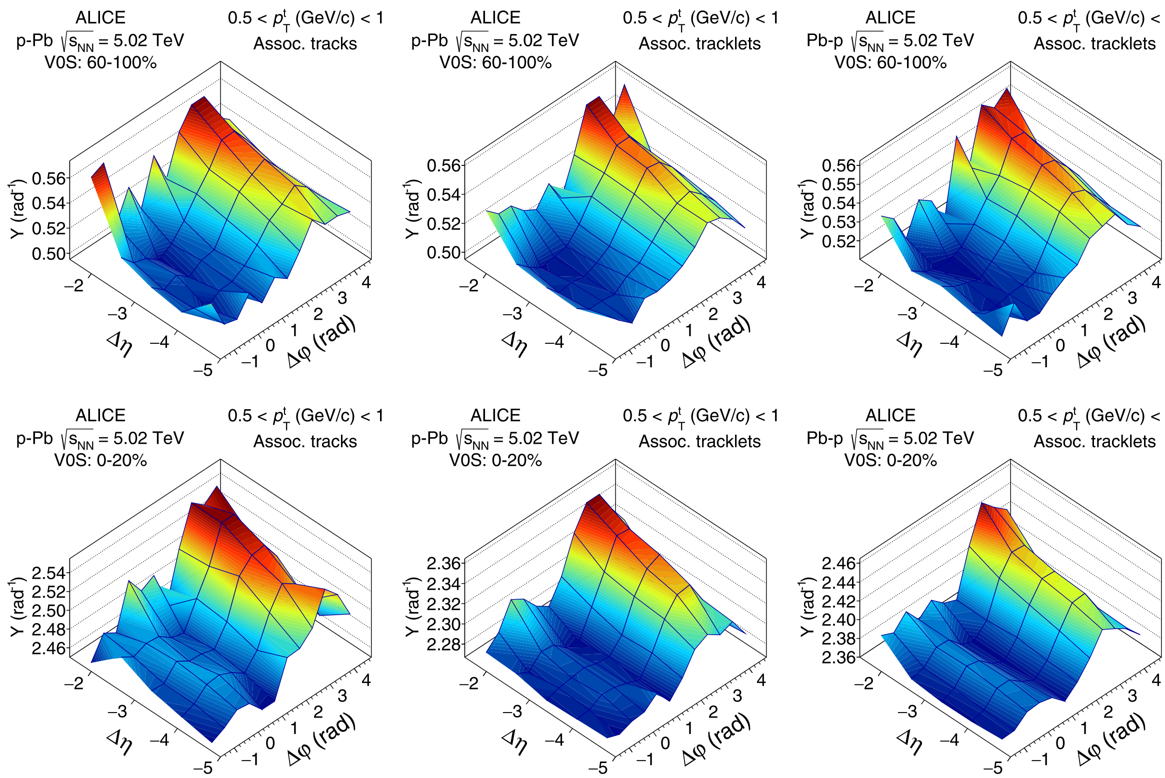


**Fig. 2.** Associated yield per trigger particle as a function of $\Delta\eta$ and $\Delta\varphi$ for muon-track correlations in p–Pb (left) and muon-tracklet correlations in p–Pb (middle) and Pb–p (right panels), measured in 60–100% (top row) and 0–20% (bottom row) event classes. The trigger particle (muon) range is $0.5 < p_T^t < 1$ GeV/$c$, the associated particle intervals are $0.5 < p_T^a < 4.0$ GeV/$c$ for tracks and $0 < \Delta\varphi_h < 5$ mrad for tracklets. Statistical uncertainties are not shown.

in azimuthal angle ($\Delta\varphi$) and pseudorapidity ($\Delta\eta$). As in previous analyses [24,33], it is defined as

$$Y = \frac{1}{N_{\mathrm{trig}}} \frac{\mathrm{d}^2 N_{\mathrm{assoc}}}{\mathrm{d}\Delta\eta \mathrm{d}\Delta\varphi} = \frac{S(\Delta\eta, \Delta\varphi)}{B(\Delta\eta, \Delta\varphi)}, \qquad (1)$$

in intervals of event multiplicity and trigger particle transverse momentum, $p_T^t$. The variable $N_{\mathrm{trig}}$ denotes the total number of trigger particles in the event class and $p_T^t$ interval, not corrected for single-muon efficiency. The signal distribution $S(\Delta\eta, \Delta\varphi) = 1/N_{\mathrm{trig}} \mathrm{d}^2 N_{\mathrm{same}}/\mathrm{d}\Delta\eta \mathrm{d}\Delta\varphi$ is the associated yield per trigger particle for particle pairs from the same event, obtained in 1 cm-wide intervals of $z_{\mathrm{vtx}}$. A correction for pair acceptance and pair efficiency is obtained by dividing by the background distribution $B(\Delta\eta, \Delta\varphi) = \alpha\ \mathrm{d}^2 N_{\mathrm{mixed}}/\mathrm{d}\Delta\eta \mathrm{d}\Delta\varphi$. The background distribution is constructed by correlating trigger particles from one event with the associated particles from other events within the same event multiplicity class and 1 cm-wide $z_{\mathrm{vtx}}$ intervals. The factor $\alpha$ is used to normalize the background distribution to unity in the $\Delta\eta$ region of maximal pair acceptance. The final per-trigger yield is obtained by calculating the average over the $z_{\mathrm{vtx}}$ intervals weighted by $N_{\mathrm{trig}}$.

In Fig. 2, the associated yield per trigger particle as a function of $\Delta\varphi$ and $\Delta\eta$ for muon-track correlations in p–Pb (left) and muon-tracklet correlations in p–Pb (middle) and Pb–p (right panels), measured in 60–100% (top row) and 0–20% (bottom row) event classes is shown. In the low-multiplicity class (60–100%), the dominant feature is the recoil jet on the away side ($\pi/2 < \Delta\varphi < 3\pi/2$). While in previous two-particle correlation studies at midrapidity [24,33] the away-side jet structure was mostly flat in $\Delta\eta$, from $\Delta\eta = -1.5$ to $\Delta\eta = -5.0$ it decreases, as expected considering the kinematics of dijets at large $\Delta\eta$. The near side ($|\Delta\varphi| < \pi/2$) shows almost no structure in $\Delta\varphi$ and $\Delta\eta$, since it is sufficiently separated from the near-side jet peak at $(\Delta\varphi, \Delta\eta) = (0, 0)$, so that no contribution from jets is expected. In the high-multiplicity (0–20%) class, the away-side jet structure is also visible, and the associated yields are considerably higher than for the low-multiplicity (60–100%) class. Moreover, in contrast to the low-multiplicity class, a near-side structure emerges, similar to that previously observed at lower pseudorapidities, revealing that the near-side ridge extends up to pseudorapidity ranges of $2.5 < |\eta| < 4$.

In order to isolate long-range correlations, we apply the same subtraction method as in previous measurements [24,33]. Jet-associated yields have only a weak multiplicity dependence [67], thus the subtraction of the low-multiplicity event class removes most of the jet-like correlations. The per-trigger yield of the 60–100% event class is subtracted from that in the 0–20% event class, and the result is presented (labelled as $Y_{\mathrm{sub}}$) in the top panels of Fig. 3. After subtraction, two similar ridges on the near and on the away side are clearly visible.

The magnitude of the contributing long-range amplitudes is quantified by extracting the Fourier coefficients from the $\Delta\varphi$ projection of the per-trigger yield distribution, after the subtraction of the low-multiplicity class, as shown in the lower panels of Fig. 3. In order to reduce the statistical fluctuations at the edges of the per-trigger yield distribution, the $\Delta\varphi$ projection is obtained from a first-order polynomial fit along $\Delta\eta$ for each $\Delta\varphi$ interval. In the p–Pb cases, the near- and away-side amplitudes are quite different, while in the Pb–p case the amplitudes on the near and away side are similar. The difference in the amplitudes of the near- and away-side ridge, which may be due to a residual jet contribution in the subtracted distribution, is taken into account in the systematic error evaluation, as explained in Sec. 5.

The Fourier coefficients are then obtained by fitting $Y_{\mathrm{sub}}$ with

$$a_0 + 2a_1 \cos(\Delta\varphi) + 2a_2 \cos(2\Delta\varphi) + 2a_3 \cos(3\Delta\varphi)\,, \qquad (2)$$

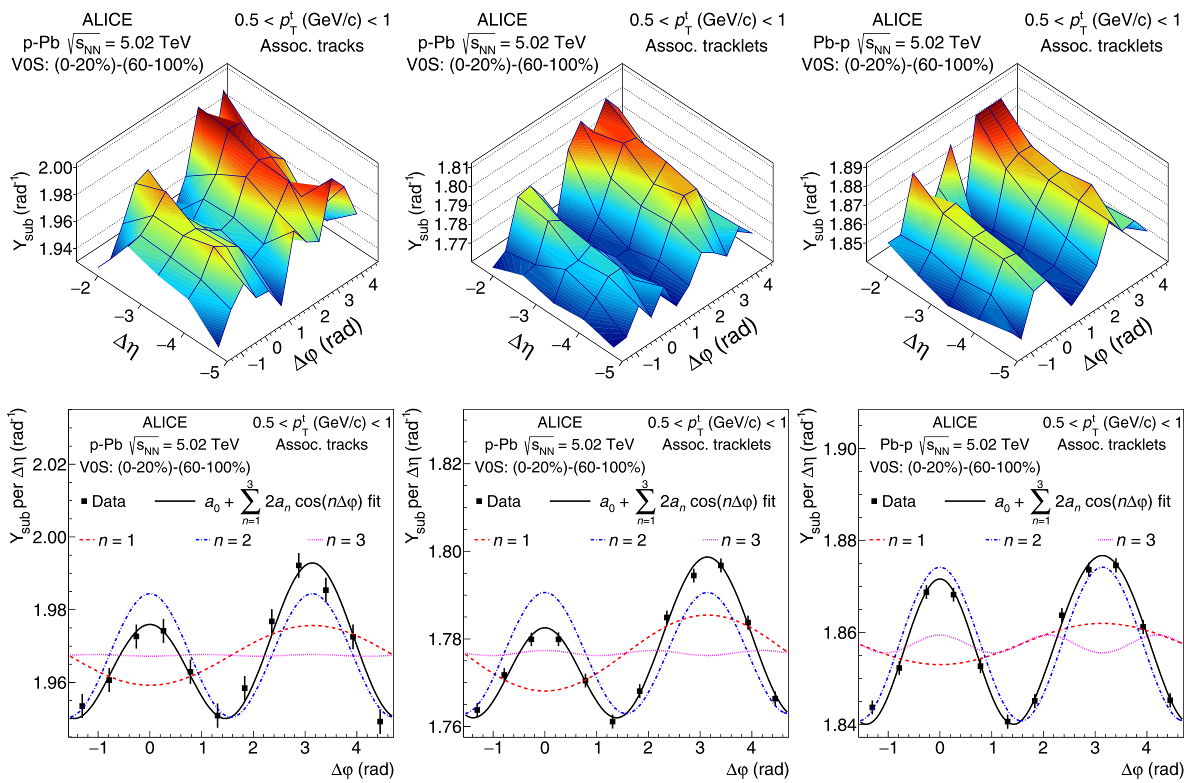


**Fig. 3.** Top panels: Associated yield per trigger particle as a function of $\Delta\varphi$ and $\Delta\eta$ for muon-track correlations in p–Pb (left) and muon-tracklet correlations in p–Pb (centre) and Pb–p (right) collisions for the 0–20% event class, where the corresponding correlation from the 60–100% event class has been subtracted. Statistical uncertainties are not shown. The trigger particle (muon) range is $0.5 < p_T^t < 1$ GeV/$c$, the associated particle intervals are $0.5 < p_T^a < 4.0$ GeV/$c$ for tracks and $0 < \Delta\varphi_h < 5$ mrad for tracklets. Bottom panels: The same as above projected onto $\Delta\varphi$. The lines indicate the fit to the data and the first harmonic contributions as explained in the text.

**Table 2**
Summary of main systematic uncertainties. The uncertainties usually depend on $p_T$ and vary within the given ranges.

| Systematic effect | Assoc. tracks | Assoc. tracklets | | |
|---|---|---|---|---|
| | p–Pb | p–Pb | Pb–p | Ratio |
| Acceptance ($z_{vtx}$ dependence) | 3–4% | 0–5% | 0–3% | 0–1% |
| Remaining jet after subtraction | 4–10% | 5–14% | 1–2% | 3–15% |
| Remaining ridge in low-multiplicity class | 1–4% | 1–6% | 0–2% | 2–8% |
| Calculation of $v_2$ | 0–1% | 0–1% | 1% | 0–2% |
| Resolution correction | 1% | 0–1% | 0–1% | 0–2% |
| Sum (added in quadrature) | 7–11% | 6–14% | 2–4% | 5–17% |

leading to $\chi^2$/NDF values typically below 1.5. The relative modulation is given by $V_{n\Delta}\{2\text{PC, sub}\} = \frac{a_n}{a_0+b}$, where $b$ is the baseline of the low-multiplicity class (60–100%) estimated from the integral of the per-trigger yield around the minimum. Assuming that the two-particle Fourier coefficient factorizes into a product of trigger and associate single-particle $v_2$ [30], the $v_n\{2\text{PC, sub}\}$ coefficients for particles reconstructed in the muon spectrometer are then obtained as

$$v_n\{2\text{PC, sub}\} = V_{n\Delta}\{2\text{PC, sub}\}/\sqrt{V^{c}_{n\Delta}\{2\text{PC, sub}\}}, \quad (3)$$

where $V^{c}_{n\Delta}\{2\text{PC, sub}\}$ is measured by correlating only central barrel tracks (or tracklets) with each other (essentially repeating the analysis as in Ref. [24]).

In this Letter, $v_2\{2\text{PC, sub}\}$ values for muons in the acceptance of the muon spectrometer are reported. Weak decays and scattering in the absorber of the muon spectrometer can cause the kinematics of reconstructed muons to deviate from those of their parent particles, and can influence the reconstructed $v_2$, especially in case $v_{2,\text{parent}}$ has a strong $p_T$ dependence. Since we cannot correct the measured $v_2$ for the species-dependent inefficiencies induced by the absorber, we denote the resulting coefficients by $v_2^{\mu}\{2\text{PC, sub}\}$ to indicate that the result holds for decay muons measured in the muon spectrometer.

## 5. Systematic uncertainties

The systematic uncertainty on $v_2^{\mu}\{2\text{PC, sub}\}$ was estimated by varying the analysis procedure as described in this section. The uncertainty on the ratio between the $v_2^{\mu}\{2\text{PC, sub}\}$ in Pb–p and p–Pb collisions was obtained on the ratio itself, in order to properly treat the (anti-) correlated systematics between the p–Pb and Pb–p data samples. A summary is given in Table 2.

The acceptance of the ALICE central barrel depends on the position of $z_{vtx}$. To study its influence on $v_2^{\mu}\{2\text{PC, sub}\}$, the analysis was repeated using only events with a reconstructed primary vertex within ±5 cm instead of ±7 cm from the nominal interaction point. The yield per trigger particle was not corrected for single track acceptance and efficiency of associated particles. Since $v_2^{\mu}\{2\text{PC, sub}\}$ is a relative quantity, it is not expected to depend on the normalization. This was verified in the case of the muon-track analysis, where good agreement was found between the second-order Fourier coefficients obtained with and without single-track acceptance and efficiency corrections. Hence, no additional uncertainty was considered.

As observed in previous analyses [24,33], the subtraction of the low-multiplicity class leads to a residual peak around $(\Delta\eta, \Delta\varphi) \approx (0, 0)$, possibly due to a bias of the event selection on the jet fragmentation in low-multiplicity events [67]. The pseudorapidity gap [24,25] used to calculate $V^{c}_{n\Delta}$ was varied from 1.2 to 1.0 and to 0.8 in order to estimate the contribution of the residual near-side short-range correlations. Due to the large gap in pseudorapidity between the ALICE central barrel and the muon spectrometer, this contribution does not affect the forward-central correlation. The effect of the bias introduced by the multiplicity selection was addressed on the away side by scaling the 60–100% multiplicity class. The scaling factor ($f$) is determined as the ratio between away-side yields in high- and low-multiplicity classes after the subtraction of the second-order Fourier component [67]. This procedure was applied in the calculation of both $V_{n\Delta}$ and $V^{c}_{n\Delta}$. The scaling factors were found to be larger in the case of p–Pb collisions ($f \leq 1.40$), compared to Pb–p ($f \leq 1.26$), and tend to be lower for increasing $p_T$. The difference with respect to the baseline results, for which no scaling ($f = 1$) is applied, was taken as the systematic uncertainty.

As previously reported [67], the contribution of the long-range correlations to the measured yields is not significant in low-multiplicity events. Still, their potential influence was addressed by changing the multiplicity range from 60–100% to 70–100% for the low-multiplicity class.

To test the stability of the fit, the $v_2$ coefficient was calculated using a fit with only the first and the second Fourier components in Eq. (2). As another variation, the baseline $b$ was calculated from a fit of the per-trigger yield in the low-multiplicity class using a Gaussian to model the shape of the away-side ridge and a constant to estimate $b$. An equivalent approach, which makes use of the baseline of the high-multiplicity class $B$ in $V_{n\Delta}\{\text{2PC, sub}\} = a_n/B$, was also used, where $B$ was estimated from the integral or from a parabolic fit of the correlation function around the minimum. Finally, the $\Delta\varphi$ projection was obtained from a weighted average instead of a first-order polynomial fit along $\Delta\eta$ for each $\Delta\varphi$ interval.

The effect from the finite angular and momentum resolution of the muon spectrometer on $v_2^{\mu}\{\text{2PC, sub}\}$ was evaluated from a dedicated MC study with the measured $v_2$ as input distribution, and resulted in a small correction of below 2%. The associated uncertainty was evaluated by varying the input $v_2$ by 50% at the lowest and highest measured points.

## 6. Results

The $v_2^{\mu}\{\text{2PC, sub}\}$ coefficients were measured for muon tracks in the p-going direction (p–Pb period) using both tracks and tracklets as associated central barrel particles, as described in Sec. 4. The $v_2^{\mu}\{\text{2PC, sub}\}$ coefficients obtained from the per-trigger yields of associated central barrel tracks agree well with those of associated tracklets, as shown in Fig. 4 as a function of muon $p_T$. Since the two measurements probe different ranges in associated particle $p_T$, the agreement is a consequence of trigger and associate $v_2$ factorization [30]. In addition, good agreement was found between the $v_2^{\mu}\{\text{2PC, sub}\}$ obtained with different cuts on $\Delta\varphi_h$ of associated tracklets (inducing a change of average $p_T$ by about 20%).

The p-going and Pb-going $v_2^{\mu}\{\text{2PC, sub}\}$ coefficients obtained using muon-tracklet correlations for the two different beam configurations (p–Pb and Pb–p) are reported in the left panel of Fig. 5 as a function of muon $p_T$. The Pb-going $v_2^{\mu}\{\text{2PC, sub}\}$ (i.e. when the

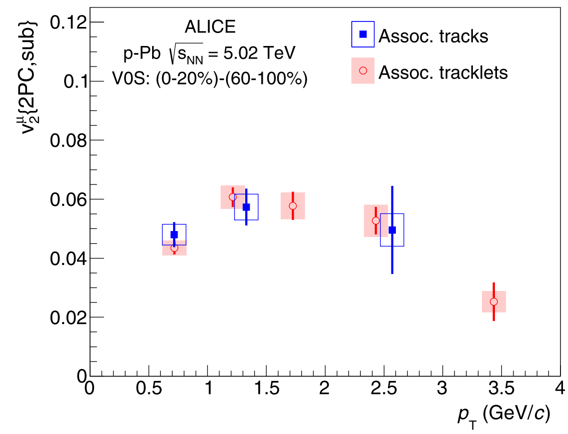


**Fig. 4.** Comparison of $v_2^{\mu}\{\text{2PC, sub}\}$ for $-4 < \eta < -2.5$ extracted from muon-track and muon-tracklet correlations in p–Pb collisions at $\sqrt{s_{NN}} = 5.02$ TeV.

muon trigger particle travels in the same direction as the Pb nucleus) is observed to be larger than the p-going $v_2^{\mu}\{\text{2PC, sub}\}$ over the measured $p_T$ range, but the two have a similar $p_T$-dependence. To quantify the asymmetry, the Pb-going over p-going ratio for the $v_2^{\mu}\{\text{2PC, sub}\}$ coefficients is reported in the right panel of Fig. 5 as a function of muon $p_T$. The ratio is found to be rather independent of $p_T$ given the statistical and systematic uncertainties of the measurement. A constant fit to the ratio adding statistical and systematic uncertainties in quadrature gives $1.16 \pm 0.06$ with a $\chi^2/\text{NDF} = 0.4$. The analysis was also repeated using the energy deposited in the neutron ZDCs on the Pb-going side instead of the V0S amplitude for the event class definition. As discussed in detail in [62], the correlation between forward energy measured in the ZDCs and particle density at central rapidities is weak in p–Pb collisions. Therefore, event classes defined as fixed fractions of the signal distribution in the ZDCs select different events, with different mean particle multiplicity at midrapidity, than the samples selected with the same fractions in the V0 detector. Still, the $v_2^{\mu}\{\text{2PC, sub}\}$ values were measured to be similar, within 25% of those extracted with V0S estimator. In addition, the asymmetry between Pb- and p-going $v_2^{\mu}\{\text{2PC, sub}\}$ was found to persist with similar shape and magnitude. The observed asymmetry may result from decorrelations of event planes at different rapidity [68].

The data in Fig. 5 cannot be readily compared with existing predictions [57] for a 3 + 1 dimensional, viscous hydrodynamical model [39] and the AMPT model with the string-melting mechanism enabled [65]. The model calculations were performed without taking into account the effect of the muon absorber, and represent the $v_2$ of primary particles, while as discussed in Sec. 3 the measured $v_2^{\mu}\{\text{2PC, sub}\}$ coefficients are reported for decay muons. Depending on particle composition and on the $p_T$-dependence of the parent particle $v_2$ distribution, the difference between primary particle $v_2$ and decay muon $v_2$ can be quite large. For example, at 1 GeV/$c$, assuming the $v_2$ of the parent particles rises with $p_T$ like at mid-rapidity [33], the measured $v_2^{\mu}\{\text{2PC, sub}\}$ for muons originating from decays of pions (kaons) would be ≈20 (40)% larger than that of the parent pions (kaons).

Instead, in Fig. 5 we show a comparison of the data with AMPT model calculations performed with the same parameters as in [57]. These calculations were performed at generator level, decaying primary particles into muons using the PYTHIA decayer [69]. The effects of the muon absorber were included by applying the $p_T$ and $\eta$ dependent relative efficiencies provided in the right panel of Fig. 1. Event characterization was done by mimicking the V0S criteria at particle level, i.e. by counting charged particles in

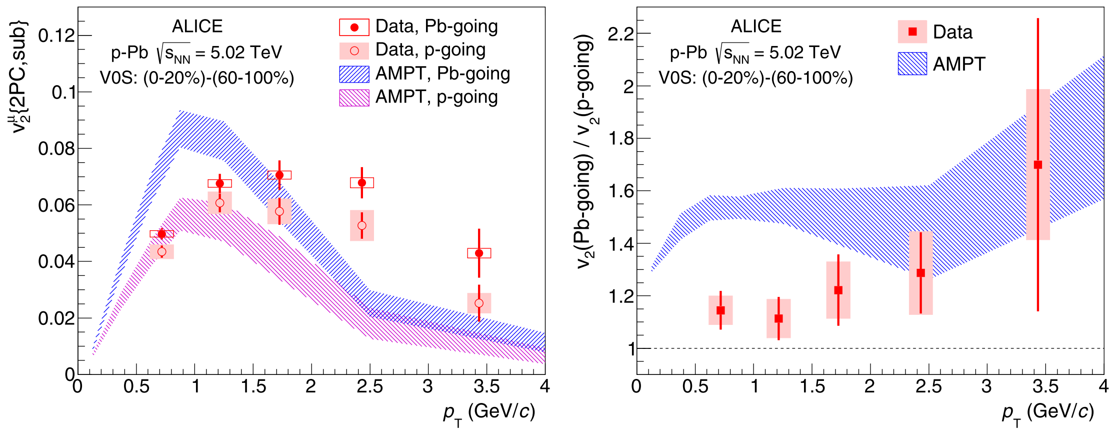


**Fig. 5.** The $v_2^{\mu}\{2\text{PC, sub}\}$ coefficients from muon-tracklet correlations in p-going and Pb-going directions (left) and their ratio (right) for $-4 < \eta < -2.5$ in p–Pb collisions at $\sqrt{s_{NN}} = 5.02$ TeV. The data are compared to model calculations from AMPT.

$2.8 < \eta < 3.9$ and $-3.7 < \eta < -2.7$. The $v_2$ values were obtained separately for muons decaying from pions, kaons and heavy-flavor hadrons, and otherwise performing the analysis in the same way as in data. We found the $v_2$ for HF muons to be consistent with zero within the generated statistics (5M events with a HF muon in the acceptance of the muon spectrometer for each period). Hence, for the inclusive $v_2$, which is obtained by weighting the calculated $v_2$ with the relative yields in each decay channel, the $v_2$ for HF muons has been set to zero to reduce statistical fluctuations. In AMPT the factor $f$ used to scale low-multiplicity class to eliminate the remaining jet contribution after subtraction, reaches values much larger than in the data, up to $f = 2$. Applying the scaling reduces the extracted $v_2$ and consequently this choice constitutes the lower (upper) bound of the shaded area in Fig. 5 left (right), while the opposite bounds correspond to $f = 1$ (as used for the baseline result in the data).

As shown in the left panel of Fig. 5, below $p_T < 1.5$ GeV/$c$, where the inclusive muon yield is expected to be dominated by weak decays of pions and kaons, the calculation produces qualitatively similar trends as observed in the data. However, quantitatively a different $p_T$ and $\eta$ dependence is found, visible in particular in the right panel of Fig. 5. At $p_T > 2$ GeV/$c$, where the inclusive muon yield is dominated by heavy-flavor decays, the data may support a finite value for the $v_2$ of HF muons, or a drastically different composition of the parent distribution or their $v_2$ values in AMPT compared to data. Indeed, comparing predictions of AMPT to pion, kaon and D-meson yields measured at midrapidity [70,71], muons from heavy-flavor decays would be underestimated by a factor 3–5 relative to pion and kaon decays assuming the same discrepancy between model and data at forward rapidity. A finite value for HF muon $v_2$ would be consistent with the emergence of radial flow in heavy-flavor meson spectra as predicted in [72], and has been recently measured in Pb–Pb collisions at $\sqrt{s_{NN}} = 2.76$ TeV [73].

## 7. Summary

Two-particle angular correlations between trigger particles in the forward pseudorapidity range $2.5 < |\eta| < 4.0$ and associated particles in the central range $|\eta| < 1.0$ measured by ALICE are reported in p–Pb collisions at a nucleon–nucleon centre-of-mass energy of 5.02 TeV. The trigger particles are inclusive muons and the associated particles are charged particles, reconstructed by the muon spectrometer and central barrel tracking detectors, respectively. The composition of parent particles for the measured muons is expected to vary as a function of $p_T$ (Fig. 1). A near-side ridge is observed in high-multiplicity events (Fig. 2). After subtraction of jet-like correlations measured in low-multiplicity events, the double-ridge structure, previously discovered in two-particle angular correlations at midrapidity, is found to persist even in the pseudorapidity ranges studied here (Fig. 3). The second-order Fourier coefficients for muon tracks are determined assuming factorization of the Fourier coefficients at central and forward rapidity. The measurement in p–Pb collisions was performed in two different ways, using tracks or tracklets for particles at $|\eta| < 1.0$, yielding consistent results (Fig. 4). The second-order Fourier coefficients for muons in high-multiplicity events were found to have a similar transverse momentum dependence in the p-going (p–Pb) and Pb-going (Pb–p) configurations, with the Pb-going coefficients larger by $16 \pm 6\%$, rather independent of $p_T$ within the uncertainties of the measurement (Fig. 5). The results were compared with calculations using the AMPT model incorporating the effects of the muon absorber, showing a different $p_T$ and $\eta$ dependence than observed in the data. Above 2 GeV/$c$, the results are sensitive to the $v_2$ of heavy-flavor decay muons. Forthcoming model calculations should apply the relative efficiencies for muon decays from pion and kaons (provided in Fig. 1) at generator level for detailed comparison with our data. Further measurements (e.g. of heavy-flavor muon yields or charged-particle $v_2$ at forward rapidity) will be needed to reduce the ambiguity between muon parent particle composition and their $v_2$.


## Acknowledgements

The ALICE Collaboration would like to thank all its engineers and technicians for their invaluable contributions to the construction of the experiment and the CERN accelerator teams for the outstanding performance of the LHC complex. The ALICE Collaboration gratefully acknowledges the resources and support provided by all Grid centres and the Worldwide LHC Computing Grid (WLCG) Collaboration. The ALICE Collaboration acknowledges the following funding agencies for their support in building and running the ALICE detector: State Committee of Science, World Federation of Scientists (WFS) and Swiss Fonds Kidagan, Armenia; Conselho Nacional de Desenvolvimento Científico e Tecnológico (CNPq), Financiadora de Estudos e Projetos (FINEP), Fundação de Amparo à Pesquisa do Estado de São Paulo (FAPESP); National Natural Science Foundation of China (NSFC), the Chinese Ministry of Education (CMOE) and the Ministry of Science and Technology of China (MSTC); Ministry of Education and Youth of the Czech Republic;

Danish Natural Science Research Council, the Carlsberg Foundation and the Danish National Research Foundation; The European Research Council under the European Community's Seventh Framework Programme; Helsinki Institute of Physics and the Academy of Finland; French CNRS-IN2P3, the 'Region Pays de Loire', 'Region Alsace', 'Region Auvergne' and CEA, France; German Bundesministerium fur Bildung, Wissenschaft, Forschung und Technologie (BMBF) and the Helmholtz Association; General Secretariat for Research and Technology, Ministry of Development, Greece; National Research, Development and Innovation Office (NKFIH), Hungary; Department of Atomic Energy and Department of Science and Technology of the Government of India; Istituto Nazionale di Fisica Nucleare (INFN) and Centro Fermi – Museo Storico della Fisica e Centro Studi e Ricerche "Enrico Fermi", Italy; Japan Society for the Promotion of Science (JSPS), KAKENHI and MEXT, Japan; Joint Institute for Nuclear Research, Dubna; National Research Foundation of Korea (NRF); Consejo Nacional de Cienca y Tecnologia (CONACYT), Direccion General de Asuntos del Personal Academico (DGAPA), México, Amerique Latine Formation academique – European Commission (ALFA-EC) and the EPLANET Program (European Particle Physics Latin American Network); Stichting voor Fundamenteel Onderzoek der Materie (FOM) and the Nederlandse Organisatie voor Wetenschappelijk Onderzoek (NWO), Netherlands; Research Council of Norway (NFR); National Science Centre, Poland; Ministry of National Education/Institute for Atomic Physics and National Council of Scientific Research in Higher Education (CNCSI-UEFISCDI), Romania; Ministry of Education and Science of Russian Federation, Russian Academy of Sciences, Russian Federal Agency of Atomic Energy, Russian Federal Agency for Science and Innovations and The Russian Foundation for Basic Research; Ministry of Education of Slovakia; Department of Science and Technology, South Africa; Centro de Investigaciones Energeticas, Medioambientales y Tecnologicas (CIEMAT), E-Infrastructure shared between Europe and Latin America (EELA), Ministerio de Economía y Competitividad (MINECO) of Spain, Xunta de Galicia (Consellería de Educación), Centro de Aplicaciones Tecnológicas y Desarrollo Nuclear (CEADEN), Cubaenergía, Cuba, and IAEA (International Atomic Energy Agency); Swedish Research Council (VR) and Knut & Alice Wallenberg Foundation (KAW); Ukraine Ministry of Education and Science; United Kingdom Science and Technology Facilities Council (STFC); The United States Department of Energy, the United States National Science Foundation, the State of Texas, and the State of Ohio; Ministry of Science, Education and Sports of Croatia and Unity through Knowledge Fund, Croatia; Council of Scientific and Industrial Research (CSIR), New Delhi, India; Pontificia Universidad Católica del Perú.

## References


[1] X.-N. Wang, Studying mini-jets via the $p_T$ dependence of the two particle correlation in azimuthal angle $\phi$, Phys. Rev. D 47 (1993) 2754–2760, arXiv:hep-ph/9306215.

[2] STAR Collaboration, J. Adams, et al., Minijet deformation and charge-independent angular correlations on momentum subspace (eta, phi) in Au–Au collisions at $\sqrt{s_{NN}} = 130$-GeV, Phys. Rev. C 73 (2006) 064907, arXiv:nucl-ex/0411003.

[3] PHOBOS Collaboration, B. Alver, et al., System size dependence of cluster properties from two-particle angular correlations in Cu+Cu and Au+Au collisions at $\sqrt{s_{NN}} = 200$ GeV, Phys. Rev. C 81 (2010) 024904, arXiv:0812.1172 [nucl-ex].

[4] PHOBOS Collaboration, B. Alver, et al., High transverse momentum triggered correlations over a large pseudorapidity acceptance in Au+Au collisions at $\sqrt{s_{NN}} = 200$ GeV, Phys. Rev. Lett. 104 (2010) 062301, arXiv:0903.2811 [nucl-ex].

[5] STAR Collaboration, B.I. Abelev, et al., Long range rapidity correlations and jet production in high energy nuclear collisions, Phys. Rev. C 80 (2009) 064912, arXiv:0909.0191 [nucl-ex].

[6] CMS Collaboration, S. Chatrchyan, et al., Long-range and short-range dihadron angular correlations in central Pb–Pb collisions at a nucleon–nucleon center of mass energy of 2.76 TeV, J. High Energy Phys. 1107 (2011) 076, arXiv:1105.2438 [nucl-ex].

[7] ALICE Collaboration, K. Aamodt, et al., Harmonic decomposition of two-particle angular correlations in Pb–Pb collisions at $\sqrt{s_{NN}} = 2.76$ TeV, Phys. Lett. B 708 (2012) 249–264, arXiv:1109.2501 [nucl-ex].

[8] STAR Collaboration, G. Agakishiev, et al., Anomalous centrality evolution of two-particle angular correlations from Au–Au collisions at $\sqrt{s_{NN}} = 62$ and 200 GeV, Phys. Rev. C 86 (2012) 064902, arXiv:1109.4380 [nucl-ex].

[9] CMS Collaboration, S. Chatrchyan, et al., Centrality dependence of dihadron correlations and azimuthal anisotropy harmonics in Pb–Pb collisions at $\sqrt{s_{NN}} = 2.76$ TeV, Eur. Phys. J. C 72 (2012) 2012, arXiv:1201.3158 [nucl-ex].

[10] ATLAS Collaboration, G. Aad, et al., Measurement of the azimuthal anisotropy for charged particle production in $\sqrt{s_{NN}} = 2.76$ TeV lead–lead collisions with the ATLAS detector, Phys. Rev. C 86 (2012) 014907, arXiv:1203.3087 [hep-ex].

[11] ALICE Collaboration, K. Aamodt, et al., Higher harmonic anisotropic flow measurements of charged particles in Pb+Pb collisions at 2.76 TeV, Phys. Rev. Lett. 107 (2011) 032301, arXiv:1105.3865 [nucl-ex].

[12] PHENIX Collaboration, A. Adare, et al., Measurements of higher-order flow harmonics in Au+Au collisions at $\sqrt{s_{NN}} = 200$ GeV, Phys. Rev. Lett. 107 (2011) 252301, arXiv:1105.3928 [nucl-ex].

[13] ALICE Collaboration, B. Abelev, et al., Anisotropic flow of charged hadrons, pions and (anti-)protons measured at high transverse momentum in Pb–Pb collisions at $\sqrt{s_{NN}} = 2.76$ TeV, Phys. Lett. B 719 (2013) 18–28, arXiv:1205.5761 [nucl-ex].

[14] CMS Collaboration, S. Chatrchyan, et al., Measurement of the azimuthal anisotropy of neutral pions in Pb–Pb collisions at $\sqrt{s_{NN}} = 2.76$ TeV, Phys. Rev. Lett. 110 (2013) 042301, arXiv:1208.2470 [nucl-ex].

[15] CMS Collaboration, S. Chatrchyan, et al., Measurement of higher-order harmonic azimuthal anisotropy in Pb–Pb collisions at $\sqrt{s_{NN}} = 2.76$ TeV, Phys. Rev. C 89 (2014) 044906, arXiv:1310.8651 [nucl-ex].

[16] ATLAS Collaboration, G. Aad, et al., Measurement of flow harmonics with multi-particle cumulants in Pb+Pb collisions at $\sqrt{s_{NN}} = 2.76$ TeV with the ATLAS detector, Eur. Phys. J. C 74 (2014) 3157, arXiv:1408.4342 [hep-ex].

[17] J.-Y. Ollitrault, Anisotropy as a signature of transverse collective flow, Phys. Rev. D 46 (1992) 229–245.

[18] B. Alver, G. Roland, Collision geometry fluctuations and triangular flow in heavy-ion collisions, Phys. Rev. C 81 (2010) 054905, arXiv:1003.0194 [nucl-th].

[19] B. Alver, C. Gombeaud, M. Luzum, J.-Y. Ollitrault, Triangular flow in hydrodynamics and transport theory, Phys. Rev. C 82 (2010) 034913, arXiv:1007.5469 [nucl-th].

[20] B. Schenke, S. Jeon, C. Gale, Elliptic and triangular flow in event-by-event $(3 + 1)$D viscous hydrodynamics, Phys. Rev. Lett. 106 (2011) 042301, arXiv:1009.3244 [hep-ph].

[21] Z. Qiu, C. Shen, U. Heinz, Hydrodynamic elliptic and triangular flow in Pb–Pb collisions at $\sqrt{s} = 2.76$ ATeV, Phys. Lett. B 707 (2012) 151–155, arXiv:1110.3033 [nucl-th].

[22] CMS Collaboration, V. Khachatryan, et al., Observation of long-range near-side angular correlations in proton–proton collisions at the LHC, J. High Energy Phys. 1009 (2010) 091, arXiv:1009.4122 [hep-ex].

[23] CMS Collaboration, S. Chatrchyan, et al., Observation of long-range near-side angular correlations in proton–lead collisions at the LHC, Phys. Lett. B 718 (2013) 795–814, arXiv:1210.5482 [nucl-ex].

[24] ALICE Collaboration, B. Abelev, et al., Long-range angular correlations on the near and away side in p–Pb collisions at $\sqrt{s_{NN}} = 5.02$ TeV, Phys. Lett. B 719 (2013) 29–41, arXiv:1212.2001 [nucl-ex].

[25] ATLAS Collaboration, G. Aad, et al., Observation of associated near-side and away-side long-range correlations in $\sqrt{s_{NN}} = 5.02$ TeV proton–lead collisions with the ATLAS detector, Phys. Rev. Lett. 110 (2013) 182302, arXiv:1212.5198 [hep-ex].

[26] PHENIX Collaboration, A. Adare, et al., Quadrupole anisotropy in dihadron azimuthal correlations in central d–Au collisions at $\sqrt{s_{NN}} = 200$ GeV, Phys. Rev. Lett. 111 (2013) 212301, arXiv:1303.1794 [nucl-ex].

[27] ATLAS Collaboration, G. Aad, et al., Measurement with the ATLAS detector of multi-particle azimuthal correlations in p–Pb collisions at $\sqrt{s_{NN}} = 5.02$ TeV, Phys. Lett. B 725 (2013) 60–78, arXiv:1303.2084 [hep-ex].

[28] CMS Collaboration, S. Chatrchyan, et al., Multiplicity and transverse momentum dependence of two- and four-particle correlations in p–Pb and Pb–Pb collisions, Phys. Lett. B 724 (2013) 213–240, arXiv:1305.0609 [nucl-ex].

[29] ALICE Collaboration, B.B. Abelev, et al., Multiparticle azimuthal correlations in p–Pb and Pb–Pb collisions at the CERN Large Hadron Collider, Phys. Rev. C 90 (5) (2014) 054901, arXiv:1406.2474 [nucl-ex].

[30] ATLAS Collaboration, G. Aad, et al., Measurement of long-range pseudorapidity correlations and azimuthal harmonics in $\sqrt{s_{NN}} = 5.02$ TeV proton–lead collisions with the ATLAS detector, Phys. Rev. C 90 (2014) 044906, arXiv:1409.1792 [hep-ex].

[31] CMS Collaboration, V. Khachatryan, et al., Evidence for collective multi-particle correlations in pPb collisions, arXiv:1502.05382 [nucl-ex].

[32] A. Bilandzic, R. Snellings, S. Voloshin, Flow analysis with cumulants: direct calculations, Phys. Rev. C 83 (2011) 044913, arXiv:1010.0233 [nucl-ex].

[33] ALICE Collaboration, B.B. Abelev, et al., Long-range angular correlations of $\pi$, K and p in p–Pb collisions at $\sqrt{s_{NN}} = 5.02$ TeV, Phys. Lett. B 726 (2013) 164–177, arXiv:1307.3237 [nucl-ex].

[34] PHENIX Collaboration, A. Adare, et al., Measurement of long-range angular correlation and quadrupole anisotropy of pions and (anti)protons in central $d$ + Au collisions at $\sqrt{s_{NN}} = 200$ GeV, Phys. Rev. Lett. 114 (2015) 192301, arXiv:1404.7461 [nucl-ex].

[35] CMS Collaboration, V. Khachatryan, et al., Long-range two-particle correlations of strange hadrons with charged particles in pPb and PbPb collisions at LHC energies, Phys. Lett. B 742 (2015) 200–224, arXiv:1409.3392 [nucl-ex].

[36] E. Avsar, C. Flensburg, Y. Hatta, J.-Y. Ollitrault, T. Ueda, Eccentricity and elliptic flow in proton–proton collisions from parton evolution, Phys. Lett. B 702 (2011) 394–397, arXiv:1009.5643 [hep-ph].

[37] K. Werner, I. Karpenko, T. Pierog, The 'ridge' in pp scattering at 7 TeV, Phys. Rev. Lett. 106 (2011) 122004, arXiv:1011.0375 [hep-ph].

[38] W.-T. Deng, Z. Xu, C. Greiner, Elliptic and triangular flow and their correlation in ultrarelativistic high multiplicity pp collisions at 14 TeV, Phys. Lett. B 711 (2012) 301–306, arXiv:1112.0470 [hep-ph].

[39] P. Bozek, Collective flow in p–Pb and d–Pb collisions at TeV energies, Phys. Rev. C 85 (2012) 014911, arXiv:1112.0915 [hep-ph].

[40] P. Bozek, W. Broniowski, Correlations from hydrodynamic flow in p–Pb collisions, Phys. Lett. B 718 (2013) 1557–1561, arXiv:1211.0845 [nucl-th].

[41] P. Bozek, W. Broniowski, Collective dynamics in high-energy proton–nucleus collisions, Phys. Rev. C 88 (2013) 014903, arXiv:1304.3044 [nucl-th].

[42] E. Shuryak, I. Zahed, High-multiplicity pp and p–A collisions: hydrodynamics at its edge, Phys. Rev. C 88 (2013) 044915, arXiv:1301.4470 [hep-ph].

[43] G. Başar, D. Teaney, Scaling relation between pA and AA collisions, Phys. Rev. C 90 (2014) 054903, arXiv:1312.6770 [nucl-th].

[44] A. Bzdak, B. Schenke, P. Tribedy, R. Venugopalan, Initial state geometry and the role of hydrodynamics in proton–proton, proton–nucleus and deuteron–nucleus collisions, Phys. Rev. C 87 (2013) 064906, arXiv:1304.3403 [nucl-th].

[45] K. Dusling, R. Venugopalan, Evidence for BFKL and saturation dynamics from dihadron spectra at the LHC, Phys. Rev. D 87 (2013) 051502, arXiv:1210.3890 [hep-ph].

[46] K. Dusling, R. Venugopalan, Explanation of systematics of CMS p–Pb high multiplicity di-hadron data at $\sqrt{s_{NN}} = 5.02$ TeV, Phys. Rev. D 87 (2013) 054014, arXiv:1211.3701 [hep-ph].

[47] Y.V. Kovchegov, D.E. Wertepny, Long-range rapidity correlations in heavy–light ion collisions, Nucl. Phys. A 906 (2013) 50–83, arXiv:1212.1195.

[48] K. Dusling, R. Venugopalan, Comparison of the color glass condensate to dihadron correlations in proton–proton and proton–nucleus collisions, Phys. Rev. D 87 (2013) 094034, arXiv:1302.7018 [hep-ph].

[49] A. Dumitru, T. Lappi, L. McLerran, Are the angular correlations in p–A collisions due to a Glasmion or Bose condensation?, Nucl. Phys. A 922 (2014) 140–149, arXiv:1310.7136 [hep-ph].

[50] B. Arbuzov, E. Boos, V. Savrin, CMS ridge effect at LHC as a manifestation of bremsstralung of gluons due to the quark–anti-quark string formation, Eur. Phys. J. C 71 (2011) 1730, arXiv:1104.1283 [hep-ph].

[51] C.-Y. Wong, Momentum kick model description of the ridge in $\Delta\varphi$–$\Delta\eta$ correlation in pp collisions at 7 TeV, Phys. Rev. C 84 (2011) 024901, arXiv:1105.5871 [hep-ph].

[52] M. Strikman, Transverse nucleon structure and multiparton interactions, Acta Phys. Pol. B 42 (2011) 2607–2630, arXiv:1112.3834 [hep-ph].

[53] S. Alderweireldt, P. Van Mechelen, Obtaining the CMS ridge effect with multiparton interactions, arXiv:1203.2048 [hep-ph].

[54] A. Bzdak, G.-L. Ma, Elliptic and triangular flow in p–Pb and peripheral Pb+Pb collisions from parton scatterings, Phys. Rev. Lett. 113 (2014) 252301, arXiv:1406.2804 [hep-ph].

[55] CMS Collaboration, S. Chatrchyan, et al., Pseudorapidity dependence of long-range two-particle correlations in p–Pb collisions with CMS, Tech. Rep. CMS-PAS-HIN-14-008, CERN, 2014.

[56] STAR Collaboration, L. Adamczyk, et al., Long-range pseudorapidity dihadron correlations in d–Au collisions at $\sqrt{s_{NN}} = 200$ GeV, Phys. Lett. B 747 (2015) 265–271, arXiv:1502.07652 [nucl-ex].

[57] P. Bozek, A. Bzdak, G.-L. Ma, Rapidity dependence of elliptic and triangular flow in proton–nucleus collisions from collective dynamics, arXiv:1503.03655 [hep-ph].

[58] ALICE Collaboration, K. Aamodt, et al., The ALICE experiment at the CERN LHC, J. Instrum. 3 (2008) S08002.

[59] ALICE Collaboration, B.B. Abelev, et al., Performance of the ALICE Experiment at the CERN LHC, Int. J. Mod. Phys. A 29 (2014) 1430044, arXiv:1402.4476 [nucl-ex].

[60] ALICE Collaboration, E. Abbas, et al., Performance of the ALICE VZERO system, J. Instrum. 8 (2013) P10016, arXiv:1306.3130 [nucl-ex].

[61] ALICE Collaboration, B. Abelev, et al., Pseudorapidity density of charged particles p–Pb collisions at $\sqrt{s_{NN}} = 5.02$ TeV, Phys. Rev. Lett. 110 (2013) 032301, arXiv:1210.3615 [nucl-ex].

[62] ALICE Collaboration, J. Adam, et al., Centrality dependence of particle production in p–Pb collisions at $\sqrt{s_{NN}} = 5.02$ TeV, Phys. Rev. C 91 (6) (2015) 064905, arXiv:1412.6828 [nucl-ex].

[63] S. Roesler, R. Engel, J. Ranft, The Monte Carlo event generator DPMJET-III, arXiv:hep-ph/0012252.

[64] R. Brun, et al., Geant detector description and simulation tool, CERN Program Library Long Write-up, W5013, 1994.

[65] Z.-W. Lin, C.M. Ko, B.-A. Li, B. Zhang, S. Pal, A multi-phase transport model for relativistic heavy ion collisions, Phys. Rev. C 72 (2005) 064901, arXiv:nucl-th/0411110.

[66] ALICE Collaboration, K. Aamodt, et al., Charged-particle multiplicity density at mid-rapidity in central Pb–Pb collisions at $\sqrt{s_{NN}} = 2.76$ TeV, Phys. Rev. Lett. 105 (2010) 252301, arXiv:1011.3916 [nucl-ex].

[67] ALICE Collaboration, B.B. Abelev, et al., Multiplicity dependence of jet-like two-particle correlations in p–Pb collisions at $\sqrt{s_{NN}} = 5.02$ TeV, Phys. Lett. B 741 (2015) 38–50, arXiv:1406.5463 [nucl-ex].

[68] CMS Collaboration, V. Khachatryan, et al., Evidence for transverse momentum and pseudorapidity dependent event plane fluctuations in PbPb and pPb collisions, Phys. Rev. C 92 (3) (2015) 034911, arXiv:1503.01692 [nucl-ex].

[69] T. Sjostrand, S. Mrenna, P.Z. Skands, PYTHIA 6.4 physics and manual, J. High Energy Phys. 0605 (2006) 026, arXiv:hep-ph/0603175.

[70] ALICE Collaboration, B.B. Abelev, et al., Multiplicity dependence of pion, kaon, proton and lambda production in p–Pb collisions at $\sqrt{s_{NN}} = 5.02$ TeV, Phys. Lett. B 728 (2014) 25–38, arXiv:1307.6796 [nucl-ex].

[71] ALICE Collaboration, B.B. Abelev, et al., Measurement of prompt $D$-meson production in p–Pb collisions at $\sqrt{s_{NN}} = 5.02$ TeV, Phys. Rev. Lett. 113 (23) (2014) 232301, arXiv:1405.3452 [nucl-ex].

[72] A.M. Sickles, Possible evidence for radial flow of heavy mesons in d–Au collisions, Phys. Lett. B 731 (2014) 51–56, arXiv:1309.6924 [nucl-th].

[73] ALICE Collaboration, J. Adam, et al., Elliptic flow of muons from heavy-flavour hadron decays at forward rapidity in Pb–Pb collisions at $\sqrt{s_{NN}} = 2.76$ TeV, arXiv:1507.03134 [nucl-ex].


## ALICE Collaboration


J. Adam [40], D. Adamová [83], M.M. Aggarwal [87], G. Aglieri Rinella [36], M. Agnello [111], N. Agrawal [48], Z. Ahammed [132], S.U. Ahn [68], I. Aimo [94,111], S. Aiola [136], M. Ajaz [16], A. Akindinov [58], S.N. Alam [132], D. Aleksandrov [100], B. Alessandro [111], D. Alexandre [102], R. Alfaro Molina [64], A. Alici [105,12], A. Alkin [3], J.R.M. Almaraz [119], J. Alme [38], T. Alt [43], S. Altinpinar [18], I. Altsybeev [131], C. Alves Garcia Prado [120], C. Andrei [78], A. Andronic [97], V. Anguelov [93], J. Anielski [54], T. Antičić [98], F. Antinori [108], P. Antonioli [105], L. Aphecetche [113], H. Appelshäuser [53], S. Arcelli [28], N. Armesto [17], R. Arnaldi [111], I.C. Arsene [22], M. Arslandok [53], B. Audurier [113], A. Augustinus [36], R. Averbeck [97], M.D. Azmi [19], M. Bach [43], A. Badalà [107], Y.W. Baek [44], S. Bagnasco [111], R. Bailhache [53], R. Bala [90], A. Baldisseri [15], F. Baltasar Dos Santos Pedrosa [36], R.C. Baral [61], A.M. Barbano [111], R. Barbera [29], F. Barile [33], G.G. Barnaföldi [135], L.S. Barnby [102], V. Barret [70], P. Bartalini [7], K. Barth [36], J. Bartke [117], E. Bartsch [53], M. Basile [28], N. Bastid [70], S. Basu [132], B. Bathen [54], G. Batigne [113], A. Batista Camejo [70], B. Batyunya [66], P.C. Batzing [22], I.G. Bearden [80], H. Beck [53], C. Bedda [111], N.K. Behera [48,49], I. Belikov [55], F. Bellini [28], H. Bello Martinez [2], R. Bellwied [122], R. Belmont [134], E. Belmont-Moreno [64], V. Belyaev [76], G. Bencedi [135], S. Beole [27], I. Berceanu [78],

A. Bercuci [78], Y. Berdnikov [85], D. Berenyi [135], R.A. Bertens [57], D. Berzano [36,27], L. Betev [36], A. Bhasin [90], I.R. Bhat [90], A.K. Bhati [87], B. Bhattacharjee [45], J. Bhom [128], L. Bianchi [122], N. Bianchi [72], C. Bianchin [134,57], J. Bielčík [40], J. Bielčíková [83], A. Bilandzic [80], R. Biswas [4], S. Biswas [79], S. Bjelogrlic [57], J.T. Blair [118], F. Blanco [10], D. Blau [100], C. Blume [53], F. Bock [93,74], A. Bogdanov [76], H. Bøggild [80], L. Boldizsár [135], M. Bombara [41], J. Book [53], H. Borel [15], A. Borissov [96], M. Borri [82], F. Bossú [65], E. Botta [27], S. Böttger [52], P. Braun-Munzinger [97], M. Bregant [120], T. Breitner [52], T.A. Broker [53], T.A. Browning [95], M. Broz [40], E.J. Brucken [46], E. Bruna [111], G.E. Bruno [33], D. Budnikov [99], H. Buesching [53], S. Bufalino [27,111], P. Buncic [36], O. Busch [128,93], Z. Buthelezi [65], J.B. Butt [16], J.T. Buxton [20], D. Caffarri [36], X. Cai [7], H. Caines [136], L. Calero Diaz [72], A. Caliva [57], E. Calvo Villar [103], P. Camerini [26], F. Carena [36], W. Carena [36], F. Carnesecchi [28], J. Castillo Castellanos [15], A.J. Castro [125], E.A.R. Casula [25], C. Cavicchioli [36], C. Ceballos Sanchez [9], J. Cepila [40], P. Cerello [111], J. Cerkala [115], B. Chang [123], S. Chapeland [36], M. Chartier [124], J.L. Charvet [15], S. Chattopadhyay [132], S. Chattopadhyay [101], V. Chelnokov [3], M. Cherney [86], C. Cheshkov [130], B. Cheynis [130], V. Chibante Barroso [36], D.D. Chinellato [121], P. Chochula [36], K. Choi [96], M. Chojnacki [80], S. Choudhury [132], P. Christakoglou [81], C.H. Christensen [80], P. Christiansen [34], T. Chujo [128], S.U. Chung [96], Z. Chunhui [57], C. Cicalo [106], L. Cifarelli [12,28], F. Cindolo [105], J. Cleymans [89], F. Colamaria [33], D. Colella [36,33,59], A. Collu [25], M. Colocci [28], G. Conesa Balbastre [71], Z. Conesa del Valle [51], M.E. Connors [136], J.G. Contreras [11,40], T.M. Cormier [84], Y. Corrales Morales [27], I. Cortés Maldonado [2], P. Cortese [32], M.R. Cosentino [120], F. Costa [36], P. Crochet [70], R. Cruz Albino [11], E. Cuautle [63], L. Cunqueiro [36], T. Dahms [92,37], A. Dainese [108], A. Danu [62], D. Das [101], I. Das [101,51], S. Das [4], A. Dash [121], S. Dash [48], S. De [120], A. De Caro [31,12], G. de Cataldo [104], J. de Cuveland [43], A. De Falco [25], D. De Gruttola [12,31], N. De Marco [111], S. De Pasquale [31], A. Deisting [97,93], A. Deloff [77], E. Dénes [135,i], G. D'Erasmo [33], D. Di Bari [33], A. Di Mauro [36], P. Di Nezza [72], M.A. Diaz Corchero [10], T. Dietel [89], P. Dillenseger [53], R. Divià [36], Ø. Djuvsland [18], A. Dobrin [57,81], T. Dobrowolski [77,i], D. Domenicis Gimenez [120], B. Dönigus [53], O. Dordic [22], T. Drozhzhova [53], A.K. Dubey [132], A. Dubla [57], L. Ducroux [130], P. Dupieux [70], R.J. Ehlers [136], D. Elia [104], H. Engel [52], B. Erazmus [36,113], I. Erdemir [53], F. Erhardt [129], D. Eschweiler [43], B. Espagnon [51], M. Estienne [113], S. Esumi [128], J. Eum [96], D. Evans [102], S. Evdokimov [112], G. Eyyubova [40], L. Fabbietti [37,92], D. Fabris [108], J. Faivre [71], A. Fantoni [72], M. Fasel [74], L. Feldkamp [54], D. Felea [62], A. Feliciello [111], G. Feofilov [131], J. Ferencei [83], A. Fernández Téllez [2], E.G. Ferreiro [17], A. Ferretti [27], A. Festanti [30], V.J.G. Feuillard [15,70], J. Figiel [117], M.A.S. Figueredo [124,120], S. Filchagin [99], D. Finogeev [56], F.M. Fionda [25], E.M. Fiore [33], M.G. Fleck [93], M. Floris [36], S. Foertsch [65], P. Foka [97], S. Fokin [100], E. Fragiacomo [110], A. Francescon [36,30], U. Frankenfeld [97], U. Fuchs [36], C. Furget [71], A. Furs [56], M. Fusco Girard [31], J.J. Gaardhøje [80], M. Gagliardi [27], A.M. Gago [103], M. Gallio [27], D.R. Gangadharan [74], P. Ganoti [88], C. Gao [7], C. Garabatos [97], E. Garcia-Solis [13], C. Gargiulo [36], P. Gasik [92,37], M. Germain [113], A. Gheata [36], M. Gheata [62,36], P. Ghosh [132], S.K. Ghosh [4], P. Gianotti [72], P. Giubellino [36,111], P. Giubilato [30], E. Gladysz-Dziadus [117], P. Glässel [93], D.M. Goméz Coral [64], A. Gomez Ramirez [52], P. González-Zamora [10], S. Gorbunov [43], L. Görlich [117], S. Gotovac [116], V. Grabski [64], L.K. Graczykowski [133], K.L. Graham [102], A. Grelli [57], A. Grigoras [36], C. Grigoras [36], V. Grigoriev [76], A. Grigoryan [1], S. Grigoryan [66], B. Grinyov [3], N. Grion [110], J.F. Grosse-Oetringhaus [36], J.-Y. Grossiord [130], R. Grosso [36], F. Guber [56], R. Guernane [71], B. Guerzoni [28], K. Gulbrandsen [80], H. Gulkanyan [1], T. Gunji [127], A. Gupta [90], R. Gupta [90], R. Haake [54], Ø. Haaland [18], C. Hadjidakis [51], M. Haiduc [62], H. Hamagaki [127], G. Hamar [135], A. Hansen [80], J.W. Harris [136], H. Hartmann [43], A. Harton [13], D. Hatzifotiadou [105], S. Hayashi [127], S.T. Heckel [53], M. Heide [54], H. Helstrup [38], A. Herghelegiu [78], G. Herrera Corral [11], B.A. Hess [35], K.F. Hetland [38], T.E. Hilden [46], H. Hillemanns [36], B. Hippolyte [55], R. Hosokawa [128], P. Hristov [36], M. Huang [18], T.J. Humanic [20], N. Hussain [45], T. Hussain [19], D. Hutter [43], D.S. Hwang [21], R. Ilkaev [99], I. Ilkiv [77], M. Inaba [128], M. Ippolitov [76,100], M. Irfan [19], M. Ivanov [97], V. Ivanov [85], V. Izucheev [112], P.M. Jacobs [74], S. Jadlovska [115], C. Jahnke [120], H.J. Jang [68], M.A. Janik [133], P.H.S.Y. Jayarathna [122], C. Jena [30], S. Jena [122], R.T. Jimenez Bustamante [97], P.G. Jones [102], H. Jung [44], A. Jusko [102], P. Kalinak [59], A. Kalweit [36], J. Kamin [53], J.H. Kang [137], V. Kaplin [76], S. Kar [132], A. Karasu Uysal [69], O. Karavichev [56], T. Karavicheva [56], L. Karayan [93,97], E. Karpechev [56], U. Kebschull [52], R. Keidel [138], D.L.D. Keijdener [57], M. Keil [36], K.H. Khan [16], M.M. Khan [19], P. Khan [101], S.A. Khan [132], A. Khanzadeev [85], Y. Kharlov [112], B. Kileng [38], B. Kim [137], D.W. Kim [44,68], D.J. Kim [123], H. Kim [137], J.S. Kim [44], M. Kim [44], M. Kim [137], S. Kim [21], T. Kim [137], S. Kirsch [43], I. Kisel [43], S. Kiselev [58], A. Kisiel [133], G. Kiss [135], J.L. Klay [6], C. Klein [53], J. Klein [36,93],

C. Klein-Bösing [54], A. Kluge [36], M.L. Knichel [93], A.G. Knospe [118], T. Kobayashi [128], C. Kobdaj [114], M. Kofarago [36], T. Kollegger [97,43], A. Kolojvari [131], V. Kondratiev [131], N. Kondratyeva [76], E. Kondratyuk [112], A. Konevskikh [56], M. Kopcik [115], M. Kour [90], C. Kouzinopoulos [36], O. Kovalenko [77], V. Kovalenko [131], M. Kowalski [117], G. Koyithatta Meethaleveedu [48], J. Kral [123], I. Králik [59], A. Kravčáková [41], M. Kretz [43], M. Krivda [102,59], F. Krizek [83], E. Kryshen [36], M. Krzewicki [43], A.M. Kubera [20], V. Kučera [83], T. Kugathasan [36], C. Kuhn [55], P.G. Kuijer [81], A. Kumar [90], J. Kumar [48], L. Kumar [87,79], P. Kurashvili [77], A. Kurepin [56], A.B. Kurepin [56], A. Kuryakin [99], S. Kushpil [83], M.J. Kweon [50], Y. Kwon [137], S.L. La Pointe [111], P. La Rocca [29], C. Lagana Fernandes [120], I. Lakomov [36], R. Langoy [42], C. Lara [52], A. Lardeux [15], A. Lattuca [27], E. Laudi [36], R. Lea [26], L. Leardini [93], G.R. Lee [102], S. Lee [137], I. Legrand [36], F. Lehas [81], R.C. Lemmon [82], V. Lenti [104], E. Leogrande [57], I. León Monzón [119], M. Leoncino [27], P. Lévai [135], S. Li [7,70], X. Li [14], J. Lien [42], R. Lietava [102], S. Lindal [22], V. Lindenstruth [43], C. Lippmann [97], M.A. Lisa [20], H.M. Ljunggren [34], D.F. Lodato [57], P.I. Loenne [18], V. Loginov [76], C. Loizides [74], X. Lopez [70], E. López Torres [9], A. Lowe [135], P. Luettig [53], M. Lunardon [30], G. Luparello [26], P.H.F.N.D. Luz [120], A. Maevskaya [56], M. Mager [36], S. Mahajan [90], S.M. Mahmood [22], A. Maire [55], R.D. Majka [136], M. Malaev [85], I. Maldonado Cervantes [63], L. Malinina [66,ii], D. Mal'Kevich [58], P. Malzacher [97], A. Mamonov [99], V. Manko [100], F. Manso [70], V. Manzari [36,104], M. Marchisone [27], J. Mareš [60], G.V. Margagliotti [26], A. Margotti [105], J. Margutti [57], A. Marín [97], C. Markert [118], M. Marquard [53], N.A. Martin [97], J. Martin Blanco [113], P. Martinengo [36], M.I. Martínez [2], G. Martínez García [113], M. Martinez Pedreira [36], Y. Martynov [3], A. Mas [120], S. Masciocchi [97], M. Masera [27], A. Masoni [106], L. Massacrier [113], A. Mastroserio [33], H. Masui [128], A. Matyja [117], C. Mayer [117], J. Mazer [125], M.A. Mazzoni [109], D. Mcdonald [122], F. Meddi [24], Y. Melikyan [76], A. Menchaca-Rocha [64], E. Meninno [31], J. Mercado Pérez [93], M. Meres [39], Y. Miake [128], M.M. Mieskolainen [46], K. Mikhaylov [66,58], L. Milano [36], J. Milosevic [22], L.M. Minervini [104,23], A. Mischke [57], A.N. Mishra [49], D. Miśkowiec [97], J. Mitra [132], C.M. Mitu [62], N. Mohammadi [57], B. Mohanty [132,79], L. Molnar [55], L. Montaño Zetina [11], E. Montes [10], M. Morando [30], D.A. Moreira De Godoy [113,54], S. Moretto [30], A. Morreale [113], A. Morsch [36], V. Muccifora [72], E. Mudnic [116], D. Mühlheim [54], S. Muhuri [132], M. Mukherjee [132], J.D. Mulligan [136], M.G. Munhoz [120], S. Murray [65], L. Musa [36], J. Musinsky [59], B.K. Nandi [48], R. Nania [105], E. Nappi [104], M.U. Naru [16], C. Nattrass [125], K. Nayak [79], T.K. Nayak [132], S. Nazarenko [99], A. Nedosekin [58], L. Nellen [63], F. Ng [122], M. Nicassio [97], M. Niculescu [62,36], J. Niedziela [36], B.S. Nielsen [80], S. Nikolaev [100], S. Nikulin [100], V. Nikulin [85], F. Noferini [105,12], P. Nomokonov [66], G. Nooren [57], J.C.C. Noris [2], J. Norman [124], A. Nyanin [100], J. Nystrand [18], H. Oeschler [93], S. Oh [136], S.K. Oh [67], A. Ohlson [36], A. Okatan [69], T. Okubo [47], L. Olah [135], J. Oleniacz [133], A.C. Oliveira Da Silva [120], M.H. Oliver [136], J. Onderwaater [97], C. Oppedisano [111], R. Orava [46], A. Ortiz Velasquez [63], A. Oskarsson [34], J. Otwinowski [117], K. Oyama [93], M. Ozdemir [53], Y. Pachmayer [93], P. Pagano [31], G. Paić [63], C. Pajares [17], S.K. Pal [132], J. Pan [134], A.K. Pandey [48], D. Pant [48], P. Papcun [115], V. Papikyan [1], G.S. Pappalardo [107], P. Pareek [49], W.J. Park [97], S. Parmar [87], A. Passfeld [54], V. Paticchio [104], R.N. Patra [132], B. Paul [101], T. Peitzmann [57], H. Pereira Da Costa [15], E. Pereira De Oliveira Filho [120], D. Peresunko [100,76], C.E. Pérez Lara [81], E. Perez Lezama [53], V. Peskov [53], Y. Pestov [5], V. Petráček [40], V. Petrov [112], M. Petrovici [78], C. Petta [29], S. Piano [110], M. Pikna [39], P. Pillot [113], O. Pinazza [105,36], L. Pinsky [122], D.B. Piyarathna [122], M. Płoskoń [74], M. Planinic [129], J. Pluta [133], S. Pochybova [135], P.L.M. Podesta-Lerma [119], M.G. Poghosyan [86,84], B. Polichtchouk [112], N. Poljak [129], W. Poonsawat [114], A. Pop [78], S. Porteboeuf-Houssais [70], J. Porter [74], J. Pospisil [83], S.K. Prasad [4], R. Preghenella [36,105], F. Prino [111], C.A. Pruneau [134], I. Pshenichnov [56], M. Puccio [111], G. Puddu [25], P. Pujahari [134], V. Punin [99], J. Putschke [134], H. Qvigstad [22], A. Rachevski [110], S. Raha [4], S. Rajput [90], J. Rak [123], A. Rakotozafindrabe [15], L. Ramello [32], F. Rami [55], R. Raniwala [91], S. Raniwala [91], S.S. Räsänen [46], B.T. Rascanu [53], D. Rathee [87], K.F. Read [125], J.S. Real [71], K. Redlich [77], R.J. Reed [134], A. Rehman [18], P. Reichelt [53], F. Reidt [93,36], X. Ren [7], R. Renfordt [53], A.R. Reolon [72], A. Reshetin [56], F. Rettig [43], J.-P. Revol [12], K. Reygers [93], V. Riabov [85], R.A. Ricci [73], T. Richert [34], M. Richter [22], P. Riedler [36], W. Riegler [36], F. Riggi [29], C. Ristea [62], A. Rivetti [111], E. Rocco [57], M. Rodríguez Cahuantzi [2], A. Rodriguez Manso [81], K. Røed [22], E. Rogochaya [66], D. Rohr [43], D. Röhrich [18], R. Romita [124], F. Ronchetti [72], L. Ronflette [113], P. Rosnet [70], A. Rossi [30,36], F. Roukoutakis [88], A. Roy [49], C. Roy [55], P. Roy [101], A.J. Rubio Montero [10], R. Rui [26], R. Russo [27], E. Ryabinkin [100], Y. Ryabov [85], A. Rybicki [117], S. Sadovsky [112], K. Šafařík [36], B. Sahlmuller [53], P. Sahoo [49], R. Sahoo [49], S. Sahoo [61], P.K. Sahu [61], J. Saini [132], S. Sakai [72], M.A. Saleh [134], C.A. Salgado [17], J. Salzwedel [20], S. Sambyal [90], V. Samsonov [85], X. Sanchez Castro [55], L. Šándor [59], A. Sandoval [64], M. Sano [128], D. Sarkar [132],

E. Scapparone[105], F. Scarlassara[30], R.P. Scharenberg[95], C. Schiaua[78], R. Schicker[93], C. Schmidt[97], H.R. Schmidt[35], S. Schuchmann[53], J. Schukraft[36], M. Schulc[40], T. Schuster[136], Y. Schutz[113,36], K. Schwarz[97], K. Schweda[97], G. Scioli[28], E. Scomparin[111], R. Scott[125], J.E. Seger[86], Y. Sekiguchi[127], D. Sekihata[47], I. Selyuzhenkov[97], K. Senosi[65], J. Seo[96,67], E. Serradilla[64,10], A. Sevcenco[62], A. Shabanov[56], A. Shabetai[113], O. Shadura[3], R. Shahoyan[36], A. Shangaraev[112], A. Sharma[90], M. Sharma[90], M. Sharma[90], N. Sharma[125,61], K. Shigaki[47], K. Shtejer[9,27], Y. Sibiriak[100], S. Siddhanta[106], K.M. Sielewicz[36], T. Siemiarczuk[77], D. Silvermyr[84,34], C. Silvestre[71], G. Simatovic[129], G. Simonetti[36], R. Singaraju[132], R. Singh[79], S. Singha[132,79], V. Singhal[132], B.C. Sinha[132], T. Sinha[101], B. Sitar[39], M. Sitta[32], T.B. Skaali[22], M. Slupecki[123], N. Smirnov[136], R.J.M. Snellings[57], T.W. Snellman[123], C. Søgaard[34], R. Soltz[75], J. Song[96], M. Song[137], Z. Song[7], F. Soramel[30], S. Sorensen[125], M. Spacek[40], E. Spiriti[72], I. Sputowska[117], M. Spyropoulou-Stassinaki[88], B.K. Srivastava[95], J. Stachel[93], I. Stan[62], G. Stefanek[77], M. Steinpreis[20], E. Stenlund[34], G. Steyn[65], J.H. Stiller[93], D. Stocco[113], P. Strmen[39], A.A.P. Suaide[120], T. Sugitate[47], C. Suire[51], M. Suleymanov[16], R. Sultanov[58], M. Šumbera[83], T.J.M. Symons[74], A. Szabo[39], A. Szanto de Toledo[120,i], I. Szarka[39], A. Szczepankiewicz[36], M. Szymanski[133], J. Takahashi[121], G.J. Tambave[18], N. Tanaka[128], M.A. Tangaro[33], J.D. Tapia Takaki[51,iii], A. Tarantola Peloni[53], M. Tarhini[51], M. Tariq[19], M.G. Tarzila[78], A. Tauro[36], G. Tejeda Muñoz[2], A. Telesca[36], K. Terasaki[127], C. Terrevoli[30,25], B. Teyssier[130], J. Thäder[74,97], D. Thomas[118], R. Tieulent[130], A.R. Timmins[122], A. Toia[53], S. Trogolo[111], V. Trubnikov[3], W.H. Trzaska[123], T. Tsuji[127], A. Tumkin[99], R. Turrisi[108], T.S. Tveter[22], K. Ullaland[18], A. Uras[130], G.L. Usai[25], A. Utrobicic[129], M. Vajzer[83], M. Vala[59], L. Valencia Palomo[70], S. Vallero[27], J. Van Der Maarel[57], J.W. Van Hoorne[36], M. van Leeuwen[57], T. Vanat[83], P. Vande Vyvre[36], D. Varga[135], A. Vargas[2], M. Vargyas[123], R. Varma[48], M. Vasileiou[88], A. Vasiliev[100], A. Vauthier[71], V. Vechernin[131], A.M. Veen[57], M. Veldhoen[57], A. Velure[18], M. Venaruzzo[73], E. Vercellin[27], S. Vergara Limón[2], R. Vernet[8], M. Verweij[134,36], L. Vickovic[116], G. Viesti[30,i], J. Viinikainen[123], Z. Vilakazi[126], O. Villalobos Baillie[102], A. Vinogradov[100], L. Vinogradov[131], Y. Vinogradov[99,i], T. Virgili[31], V. Vislavicius[34], Y.P. Viyogi[132], A. Vodopyanov[66], M.A. Völkl[93], K. Voloshin[58], S.A. Voloshin[134], G. Volpe[135,36], B. von Haller[36], I. Vorobyev[37,92], D. Vranic[36,97], J. Vrláková[41], B. Vulpescu[70], A. Vyushin[99], B. Wagner[18], J. Wagner[97], H. Wang[57], M. Wang[7,113], Y. Wang[93], D. Watanabe[128], Y. Watanabe[127], M. Weber[36], S.G. Weber[97], J.P. Wessels[54], U. Westerhoff[54], J. Wiechula[35], J. Wikne[22], M. Wilde[54], G. Wilk[77], J. Wilkinson[93], M.C.S. Williams[105], B. Windelband[93], M. Winn[93], C.G. Yaldo[134], H. Yang[57], P. Yang[7], S. Yano[47], Z. Yin[7], H. Yokoyama[128], I.-K. Yoo[96], V. Yurchenko[3], I. Yushmanov[100], A. Zaborowska[133], V. Zaccolo[80], A. Zaman[16], C. Zampolli[105], H.J.C. Zanoli[120], S. Zaporozhets[66], N. Zardoshti[102], A. Zarochentsev[131], P. Závada[60], N. Zaviyalov[99], H. Zbroszczyk[133], I.S. Zgura[62], M. Zhalov[85], H. Zhang[18,7], X. Zhang[74], Y. Zhang[7], C. Zhao[22], N. Zhigareva[58], D. Zhou[7], Y. Zhou[80,57], Z. Zhou[18], H. Zhu[18,7], J. Zhu[113,7], X. Zhu[7], A. Zichichi[12,28], A. Zimmermann[93], M.B. Zimmermann[54,36], G. Zinovjev[3], M. Zyzak[43]

[1] *A.I. Alikhanyan National Science Laboratory (Yerevan Physics Institute) Foundation, Yerevan, Armenia*
[2] *Benemérita Universidad Autónoma de Puebla, Puebla, Mexico*
[3] *Bogolyubov Institute for Theoretical Physics, Kiev, Ukraine*
[4] *Bose Institute, Department of Physics and Centre for Astroparticle Physics and Space Science (CAPSS), Kolkata, India*
[5] *Budker Institute for Nuclear Physics, Novosibirsk, Russia*
[6] *California Polytechnic State University, San Luis Obispo, CA, United States*
[7] *Central China Normal University, Wuhan, China*
[8] *Centre de Calcul de l'IN2P3, Villeurbanne, France*
[9] *Centro de Aplicaciones Tecnológicas y Desarrollo Nuclear (CEADEN), Havana, Cuba*
[10] *Centro de Investigaciones Energéticas Medioambientales y Tecnológicas (CIEMAT), Madrid, Spain*
[11] *Centro de Investigación y de Estudios Avanzados (CINVESTAV), Mexico City and Mérida, Mexico*
[12] *Centro Fermi – Museo Storico della Fisica e Centro Studi e Ricerche "Enrico Fermi", Rome, Italy*
[13] *Chicago State University, Chicago, IL, USA*
[14] *China Institute of Atomic Energy, Beijing, China*
[15] *Commissariat à l'Energie Atomique, IRFU, Saclay, France*
[16] *COMSATS Institute of Information Technology (CIIT), Islamabad, Pakistan*
[17] *Departamento de Física de Partículas and IGFAE, Universidad de Santiago de Compostela, Santiago de Compostela, Spain*
[18] *Department of Physics and Technology, University of Bergen, Bergen, Norway*
[19] *Department of Physics, Aligarh Muslim University, Aligarh, India*
[20] *Department of Physics, Ohio State University, Columbus, OH, United States*
[21] *Department of Physics, Sejong University, Seoul, South Korea*
[22] *Department of Physics, University of Oslo, Oslo, Norway*
[23] *Dipartimento di Elettrotecnica ed Elettronica del Politecnico, Bari, Italy*
[24] *Dipartimento di Fisica dell'Università 'La Sapienza' and Sezione INFN Rome, Italy*
[25] *Dipartimento di Fisica dell'Università and Sezione INFN, Cagliari, Italy*

[26] *Dipartimento di Fisica dell'Università and Sezione INFN, Trieste, Italy*
[27] *Dipartimento di Fisica dell'Università and Sezione INFN, Turin, Italy*
[28] *Dipartimento di Fisica e Astronomia dell'Università and Sezione INFN, Bologna, Italy*
[29] *Dipartimento di Fisica e Astronomia dell'Università and Sezione INFN, Catania, Italy*
[30] *Dipartimento di Fisica e Astronomia dell'Università and Sezione INFN, Padova, Italy*
[31] *Dipartimento di Fisica 'E.R. Caianiello' dell'Università and Gruppo Collegato INFN, Salerno, Italy*
[32] *Dipartimento di Scienze e Innovazione Tecnologica dell'Università del Piemonte Orientale and Gruppo Collegato INFN, Alessandria, Italy*
[33] *Dipartimento Interateneo di Fisica 'M. Merlin' and Sezione INFN, Bari, Italy*
[34] *Division of Experimental High Energy Physics, University of Lund, Lund, Sweden*
[35] *Eberhard Karls Universität Tübingen, Tübingen, Germany*
[36] *European Organization for Nuclear Research (CERN), Geneva, Switzerland*
[37] *Excellence Cluster Universe, Technische Universität München, Munich, Germany*
[38] *Faculty of Engineering, Bergen University College, Bergen, Norway*
[39] *Faculty of Mathematics, Physics and Informatics, Comenius University, Bratislava, Slovakia*
[40] *Faculty of Nuclear Sciences and Physical Engineering, Czech Technical University in Prague, Prague, Czech Republic*
[41] *Faculty of Science, P.J. Šafárik University, Košice, Slovakia*
[42] *Faculty of Technology, Buskerud and Vestfold University College, Vestfold, Norway*
[43] *Frankfurt Institute for Advanced Studies, Johann Wolfgang Goethe-Universität Frankfurt, Frankfurt, Germany*
[44] *Gangneung-Wonju National University, Gangneung, South Korea*
[45] *Gauhati University, Department of Physics, Guwahati, India*
[46] *Helsinki Institute of Physics (HIP), Helsinki, Finland*
[47] *Hiroshima University, Hiroshima, Japan*
[48] *Indian Institute of Technology Bombay (IIT), Mumbai, India*
[49] *Indian Institute of Technology Indore, Indore (IITI), India*
[50] *Inha University, Incheon, South Korea*
[51] *Institut de Physique Nucléaire d'Orsay (IPNO), Université Paris-Sud, CNRS-IN2P3, Orsay, France*
[52] *Institut für Informatik, Johann Wolfgang Goethe-Universität Frankfurt, Frankfurt, Germany*
[53] *Institut für Kernphysik, Johann Wolfgang Goethe-Universität Frankfurt, Frankfurt, Germany*
[54] *Institut für Kernphysik, Westfälische Wilhelms-Universität Münster, Münster, Germany*
[55] *Institut Pluridisciplinaire Hubert Curien (IPHC), Université de Strasbourg, CNRS-IN2P3, Strasbourg, France*
[56] *Institute for Nuclear Research, Academy of Sciences, Moscow, Russia*
[57] *Institute for Subatomic Physics of Utrecht University, Utrecht, Netherlands*
[58] *Institute for Theoretical and Experimental Physics, Moscow, Russia*
[59] *Institute of Experimental Physics, Slovak Academy of Sciences, Košice, Slovakia*
[60] *Institute of Physics, Academy of Sciences of the Czech Republic, Prague, Czech Republic*
[61] *Institute of Physics, Bhubaneswar, India*
[62] *Institute of Space Science (ISS), Bucharest, Romania*
[63] *Instituto de Ciencias Nucleares, Universidad Nacional Autónoma de México, Mexico City, Mexico*
[64] *Instituto de Física, Universidad Nacional Autónoma de México, Mexico City, Mexico*
[65] *iThemba LABS, National Research Foundation, Somerset West, South Africa*
[66] *Joint Institute for Nuclear Research (JINR), Dubna, Russia*
[67] *Konkuk University, Seoul, South Korea*
[68] *Korea Institute of Science and Technology Information, Daejeon, South Korea*
[69] *KTO Karatay University, Konya, Turkey*
[70] *Laboratoire de Physique Corpusculaire (LPC), Clermont Université, Université Blaise Pascal, CNRS-IN2P3, Clermont-Ferrand, France*
[71] *Laboratoire de Physique Subatomique et de Cosmologie, Université Grenoble-Alpes, CNRS-IN2P3, Grenoble, France*
[72] *Laboratori Nazionali di Frascati, INFN, Frascati, Italy*
[73] *Laboratori Nazionali di Legnaro, INFN, Legnaro, Italy*
[74] *Lawrence Berkeley National Laboratory, Berkeley, CA, United States*
[75] *Lawrence Livermore National Laboratory, Livermore, CA, United States*
[76] *Moscow Engineering Physics Institute, Moscow, Russia*
[77] *National Centre for Nuclear Studies, Warsaw, Poland*
[78] *National Institute for Physics and Nuclear Engineering, Bucharest, Romania*
[79] *National Institute of Science Education and Research, Bhubaneswar, India*
[80] *Niels Bohr Institute, University of Copenhagen, Copenhagen, Denmark*
[81] *Nikhef, Nationaal instituut voor subatomaire fysica, Amsterdam, Netherlands*
[82] *Nuclear Physics Group, STFC Daresbury Laboratory, Daresbury, United Kingdom*
[83] *Nuclear Physics Institute, Academy of Sciences of the Czech Republic, Řež u Prahy, Czech Republic*
[84] *Oak Ridge National Laboratory, Oak Ridge, TN, United States*
[85] *Petersburg Nuclear Physics Institute, Gatchina, Russia*
[86] *Physics Department, Creighton University, Omaha, NE, United States*
[87] *Physics Department, Panjab University, Chandigarh, India*
[88] *Physics Department, University of Athens, Athens, Greece*
[89] *Physics Department, University of Cape Town, Cape Town, South Africa*
[90] *Physics Department, University of Jammu, Jammu, India*
[91] *Physics Department, University of Rajasthan, Jaipur, India*
[92] *Physik Department, Technische Universität München, Munich, Germany*
[93] *Physikalisches Institut, Ruprecht-Karls-Universität Heidelberg, Heidelberg, Germany*
[94] *Politecnico di Torino, Turin, Italy*
[95] *Purdue University, West Lafayette, IN, United States*
[96] *Pusan National University, Pusan, South Korea*
[97] *Research Division and ExtreMe Matter Institute EMMI, GSI Helmholtzzentrum für Schwerionenforschung, Darmstadt, Germany*
[98] *Rudjer Bošković Institute, Zagreb, Croatia*
[99] *Russian Federal Nuclear Center (VNIIEF), Sarov, Russia*
[100] *Russian Research Centre Kurchatov Institute, Moscow, Russia*
[101] *Saha Institute of Nuclear Physics, Kolkata, India*
[102] *School of Physics and Astronomy, University of Birmingham, Birmingham, United Kingdom*
[103] *Sección Física, Departamento de Ciencias, Pontificia Universidad Católica del Perú, Lima, Peru*
[104] *Sezione INFN, Bari, Italy*

[105] *Sezione INFN, Bologna, Italy*
[106] *Sezione INFN, Cagliari, Italy*
[107] *Sezione INFN, Catania, Italy*
[108] *Sezione INFN, Padova, Italy*
[109] *Sezione INFN, Rome, Italy*
[110] *Sezione INFN, Trieste, Italy*
[111] *Sezione INFN, Turin, Italy*
[112] *SSC IHEP of NRC Kurchatov institute, Protvino, Russia*
[113] *SUBATECH, Ecole des Mines de Nantes, Université de Nantes, CNRS-IN2P3, Nantes, France*
[114] *Suranaree University of Technology, Nakhon Ratchasima, Thailand*
[115] *Technical University of Košice, Košice, Slovakia*
[116] *Technical University of Split FESB, Split, Croatia*
[117] *The Henryk Niewodniczanski Institute of Nuclear Physics, Polish Academy of Sciences, Cracow, Poland*
[118] *The University of Texas at Austin, Physics Department, Austin, TX, USA*
[119] *Universidad Autónoma de Sinaloa, Culiacán, Mexico*
[120] *Universidade de São Paulo (USP), São Paulo, Brazil*
[121] *Universidade Estadual de Campinas (UNICAMP), Campinas, Brazil*
[122] *University of Houston, Houston, TX, United States*
[123] *University of Jyväskylä, Jyväskylä, Finland*
[124] *University of Liverpool, Liverpool, United Kingdom*
[125] *University of Tennessee, Knoxville, TN, United States*
[126] *University of the Witwatersrand, Johannesburg, South Africa*
[127] *University of Tokyo, Tokyo, Japan*
[128] *University of Tsukuba, Tsukuba, Japan*
[129] *University of Zagreb, Zagreb, Croatia*
[130] *Université de Lyon, Université Lyon 1, CNRS/IN2P3, IPN-Lyon, Villeurbanne, France*
[131] *V. Fock Institute for Physics, St. Petersburg State University, St. Petersburg, Russia*
[132] *Variable Energy Cyclotron Centre, Kolkata, India*
[133] *Warsaw University of Technology, Warsaw, Poland*
[134] *Wayne State University, Detroit, MI, United States*
[135] *Wigner Research Centre for Physics, Hungarian Academy of Sciences, Budapest, Hungary*
[136] *Yale University, New Haven, CT, United States*
[137] *Yonsei University, Seoul, South Korea*
[138] *Zentrum für Technologietransfer und Telekommunikation (ZTT), Fachhochschule Worms, Worms, Germany*

[i] Deceased.
[ii] Also at: M.V. Lomonosov Moscow State University, D.V. Skobeltsyn Institute of Nuclear Physics, Moscow, Russia.
[iii] Also at: University of Kansas, Lawrence, Kansas, United States.